Appendix B
Russian River Watershed Climate and Hydrology

Appendix B. Russian River Watershed Climate and Hydrology

B.1 Purpose and Scope

This technical memorandum highlights the development of climate and hydrological metrics to support the Russian River Watershed Resilience Pilot (Pilot). Figure B-1 shows the study area for the Pilot, which encompasses the entirety of the Russian River watershed as well as additional Sonoma Water service areas where Russian River water supplies play a significant role in meeting urban water demands and help to offset groundwater pumping in these areas.

Figure B-1. Russian River Watershed Resilience Pilot Study Area

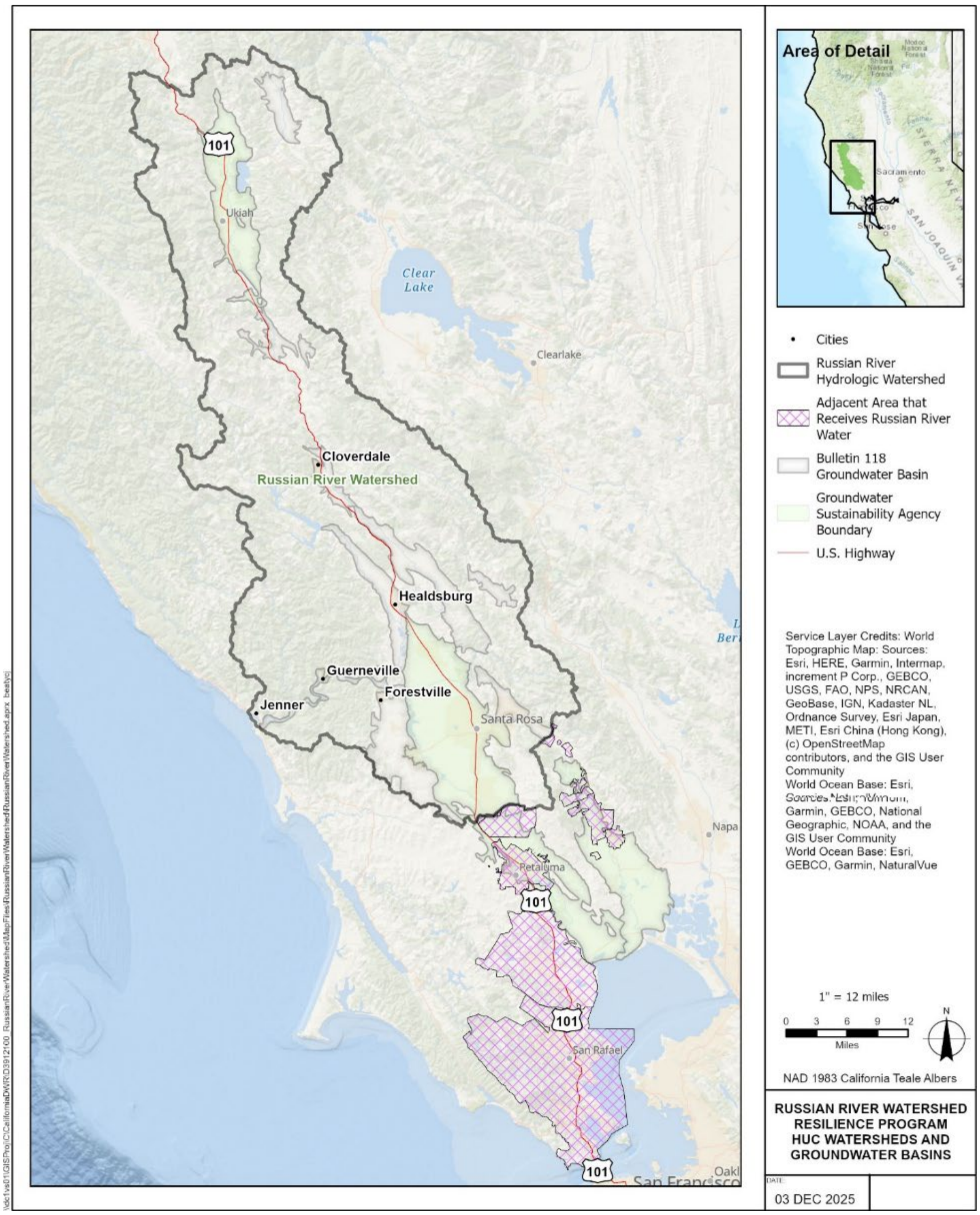

B.2 Historical Climate Overview

The Russian River watershed is experiencing a clear trend of increasing climate hazards. Rising temperatures and greater variability in precipitation are contributing to more frequent and intense floods and wildfires, prolonged droughts, and significant disruptions to water resources and ecosystems. The watershed has repeatedly experienced repeated "weather whiplash"—rapid shifts between extreme wet and dry periods—resulting in some of the most intense floods and droughts in California's history. These shifts are becoming more pronounced with climate change, amplifying risks to infrastructure, water supply, and ecological systems.

B.2.1 Paleo-Reconstruction

Tree-ring reconstructions were used to extend the historical record of Russian River Valley streamflow back to 1582, providing a long-term perspective on hydrologic variability prior to the instrumental period. These reconstructions are based on correlations between annual ring-width patterns in moisture-sensitive tree species and observed streamflow, allowing for estimation of past droughts, wet periods, and multi-decadal trends. The resulting 423-year record (1582–2004) captures a wide range of hydrologic extremes and enhances understanding of natural climate variability relevant to water-resource planning and resilience assessments (Woodhouse and Griffin 2008). Figure B-2 shows the total flow at Healdsburg for paleo-reconstruction records from 1582 to 2004. The paleo-reconstruction period exhibits a median flow of about 897 thousand acre-feet (TAF), with a wide range from 0 to 2,188 TAF, reflecting natural climate variability and episodes of both severe drought and major flood years.

Figure B-2. The Total Flow at Healdsburg for Paleo-reconstruction Records (1582–2004)

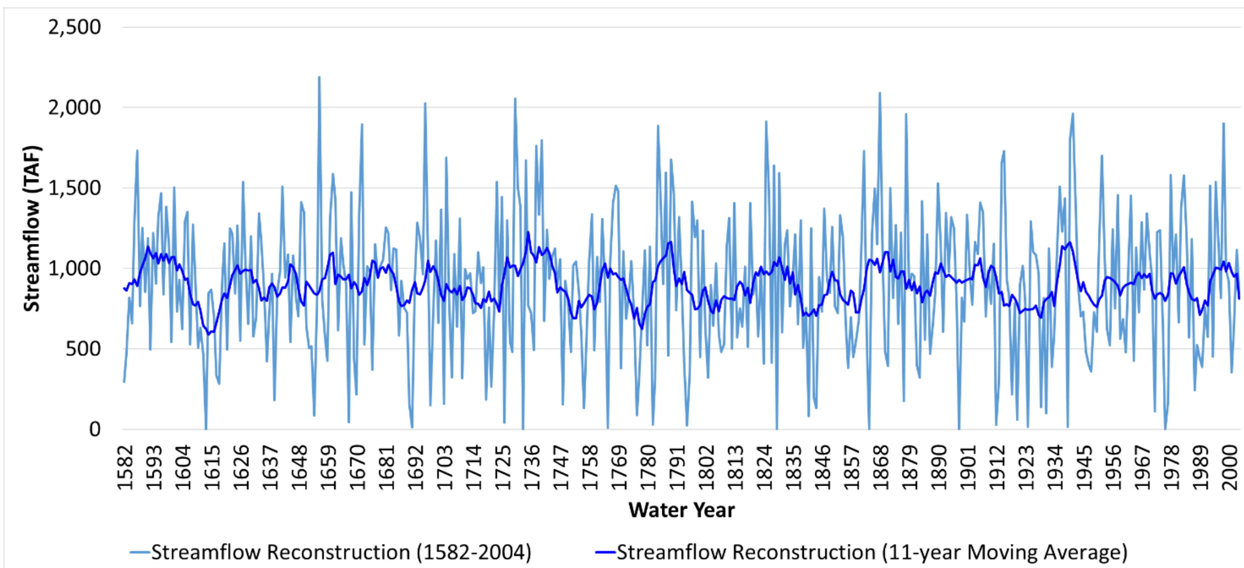

B.2.2 Instrumental Historical Climate Observations

The historical average temperature record for the Russian River hydrological domain from 1911 to 2024 shows a long-term warming trend, despite considerable year-to-year variability (Figure B-3). Annual temperatures generally fluctuate between about 55°F and 60°F, with a long-term average of around 58°F. The 11-year moving average reveals periods of relative warming in the 1930s and 1940s, followed by a cooler phase through the mid-20th century. The warmest years appear clustered after 2000, indicating that the region has experienced more frequent and sustained warm temperature conditions in the

21st century. Overall, the record reflects a gradual but notable increase in observed average temperatures over the past century.

Figure B-3. Historical Average Temperature over the Russian River Hydrological Domain from 1911 to 2024

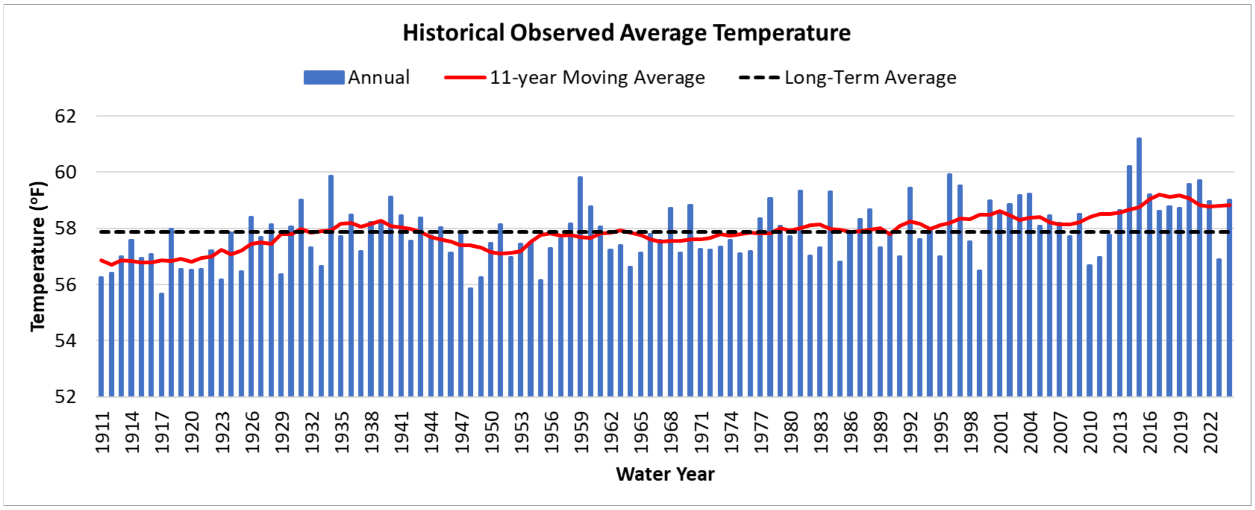

The historical precipitation record for the Russian River hydrological domain from 1911 to 2024 shows substantial year-to-year variability, characteristic of the region's highly dynamic climate (Figure B-4). Annual precipitation fluctuates widely for the region with less than 20 inches for drought years to extremely wet years exceeding 70 inches. The long-term average remains close to 43 inches. The 11-year moving average highlights multi-decadal oscillations, indicating a generally wetter period in the early 20th century that gradually transitioned into drier conditions throughout the mid-century, followed by a modest rebound in the 1980s and 1990s. In recent decades, the moving average shows heightened variability rather than a clear trend, reflecting the increasing frequency of both very dry and very wet years.

Figure B-4. Historical Precipitation over the Russian River Hydrological Domain from 1911 to 2024

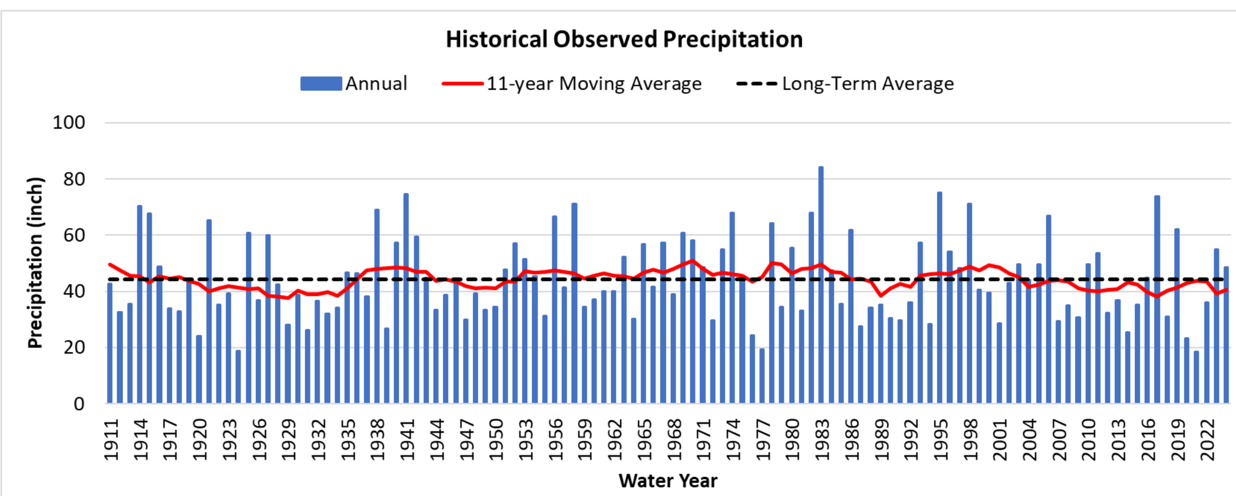

The historical record of observed total flow at Healdsburg from 1911 to 2024 shows substantial interannual variability, reflecting the region's sensitivity to swings in precipitation and hydrologic conditions (Figure B-5). Annual flows show wide range of fluctuation from extremely dry years with less than 200 TAF to exceptionally wet years exceeding 2,000 TAF. The long-term average remains close to

1,000 TAF. The 11-year moving average highlights multi-decadal shifts, with relatively high flows in the 1930s and early 1940s followed by a sustained period of lower-than-average flows through the 1950s and 1960s. Flow conditions generally stabilized near the long-term average from the late 1970s through the early 2000s, though the record also shows several sharp peaks associated with major storm years. In more recent decades, the moving average exhibits notable variability but no strong directional trend, mirroring the alternating patterns of severe drought and intense wet years that have characterized the 21st century.

Figure B-5. Historical Total Flow at Healdsburg from 1911 to 2024

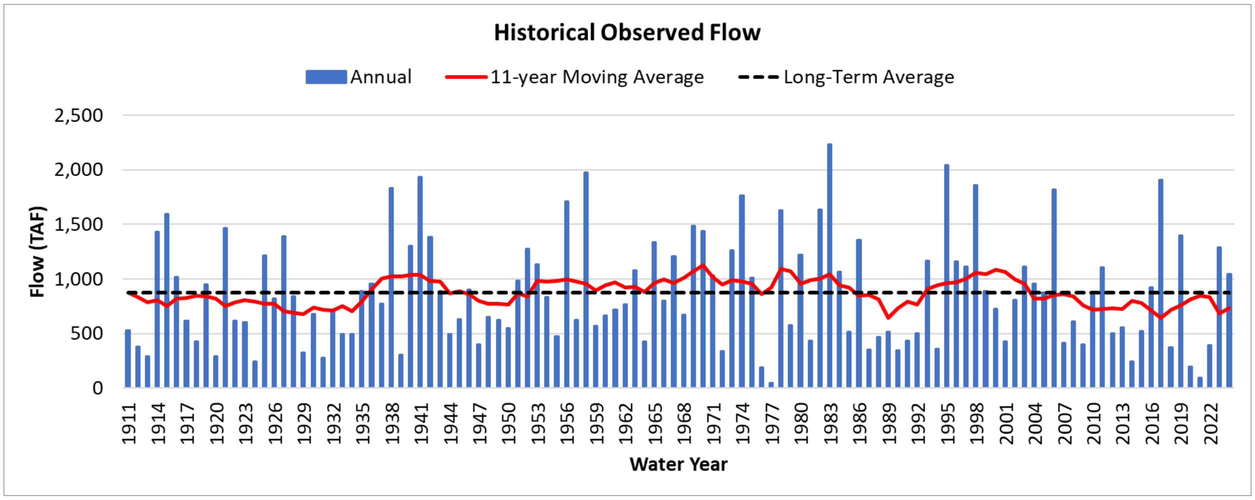

Major weather-related events have occurred in the Russian River watershed in recent decades. These events include major droughts, floods, wildfires, and extreme temperatures that impacted the water resources of the watershed. The watershed has repeatedly experienced repeated “weather whiplash”—rapid shifts between extreme wet and dry periods—resulting in some of the most intense floods and droughts in California’s history. This is the signature of historical climate in the watershed and likely continued and expanded variability in the future.

Atmospheric rivers (ARs) are the primary driver of major flooding in the Russian River watershed. All major Russian River floods in recent decades, including the catastrophic events of 1986, 1995, 2006, and 2019, have been linked to AR conditions, which account for over 99% of flood damages in Sonoma County (Sonoma Countywide Flood Risk Management Assessment 2024; CW3E 2021). The Russian River watershed has also experienced several significant wildfires in recent years, including the Mendocino Complex Fires, Kincade Fire, Sonoma Complex Fires, Walbridge Fire, and Glass Fire. These events have had profound impacts on water quality, infrastructure, and ecosystems. The Russian River watershed is especially susceptible to temperature extremes, largely because of its dependence on agriculture. In addition to acute heat waves, chronic warming trends are evident: the region now experiences more days above 100°F than in past decades, and most of the top 10 hottest July–September periods on record have occurred within the last 20 years (California Department of Insurance 2024). The Russian River watershed is also highly vulnerable to extreme drought, which poses significant challenges to both water availability and quality. Droughts in this region develop gradually over multi-year periods, with recent severe events occurring from 2012–2016 and 2020–2022, and historical droughts recorded in 1976–1977, 1987–1992, 2007–2009, and 2012–2016.

B.3 Future Climate and Hydrologic Assessments

The evaluation of climate vulnerability relies on existing data sets of the main drivers of climate change effects, primarily projected changes in temperature and changes in precipitation under future climate change conditions. In addition, anticipated hydrological responses to these climatic changes such as flooding, drought, and wildfire risks are derived from Basin Characterization Model (BCM) modeling and existing sources including Cal-Adapt, California Department of Water Resources climate change studies, and California climate change assessments. The vulnerability metrics are based on the spatial average of the hydrological boundary of the Russian River watershed. The vulnerability types consist of changes in the following areas: temperature, precipitation, runoff, drought, flooding, and wildfire (Table B-1).

Table B-1. Details of the Climatic and Hydrologic Vulnerability Metrics

S. No.	Climatic/ Hydrologic Metrics	Definition	Period	Analysis Period
C1	Temperature	Projected change in annual average temperature (°F)	Annual	Historical: 1981 to 2010 Mid Future: 2041 to 2070 Late Future: 2071 to 2100
C2	Extreme Heat Days	Projected change in number of extreme heat days per year when daily maximum temperature is above 95°F (days/yr)	Annual	Historical: 1981 to 2010 Mid Future: 2041 to 2070 Late Future: 2071 to 2100
C3	Precipitation	Projected change in annual precipitation (%)	Annual	Historical: 1981 to 2010 Mid Future: 2041 to 2070 Late Future: 2071 to 2100
C4	Extreme Precipitation	Projected change in 1% annual exceedance probability precipitation (%)	Annual	Historical: 1981 to 2010 Mid Future: 2041 to 2070 Late Future: 2071 to 2100
H1	Runoff	Projected change in annual total runoff (runoff + recharge) (%)	Annual	Historical: 1981 to 2010 Mid Future: 2041 to 2070 Late Future: 2071 to 2100
H2	Floods	Projected changes in 1% AEP flows based on 1-day and 3-day unimpaired flow (%)	Annual	Historical: 1961 to 2010 Mid Future: 2016 to 2065 Late Future: 2051 to 2100
H3	Drought	Projected change in maximum cumulative annual deficit value based on total flow (%)	Annual	Historical: 1961 to 2010 Mid Future: 2016 to 2065 Late Future: 2051 to 2100
H4	Wildfire	Projected changes for estimated decadal wildfire probabilities (%)	Decadal	Historical: 1981 to 2010 Mid Future: 2041 to 2070 Late Future: 2071 to 2100
H5	Streamflow Timing	Projected changes in the date of the year when 50% of the water-year flow has been passed (days)	Annual	Historical: 1981 to 2010 Mid Future: 2041 to 2070 Late Future: 2071 to 2100

S. No.	Climatic/ Hydrologic Metrics	Definition	Period	Analysis Period
H6	Climate Water Deficit	Projected change in the difference between PET (Potential ET) and AET (Actual ET) (%)	Annual	Historical: 1981 to 2010 Mid Future: 2041 to 2070 Late Future: 2071 to 2100
H7	Soil Moisture	Projected change in soil moisture during July and August (%)	June to August	Historical: 1981 to 2010 Mid Future: 2041 to 2070 Late Future: 2071 to 2100

Notes:

Climate and hydrological metrics were estimated using the 30-year period, whereas extreme event metrics (flood and drought) were evaluated using the 50-year period.

AEP = annual exceedance probability

The evaluation of climate and hydrological metrics was performed using the 41 climate model projections from the Coupled Model Intercomparison Project Phase 6 (CMIP6) dataset. CMIP6 represents a significant advancement in climate modeling, building on the successes of previous phases. Localized Constructed Analogs version 2 (LOCA2) improves upon the original LOCA downscaling method by offering higher spatial resolution and incorporating more sophisticated methods. While LOCA provides downscaled climate projections at a 6-kilometer (km) resolution for most of North America, LOCA2 enhances this with a 3 km resolution specifically for California, known as LOCA2-Hybrid. The LOCA2-Hybrid dataset uses 15 GCMs that performed well over California (Pierce et al. 2023). Shared Socioeconomic Pathways (SSPs) are scenarios used in climate research to explore how global societal trends might influence future greenhouse gas emissions and climate change. SSPs range from sustainable development (SSP1) to high challenges for mitigation and adaptation (SSP5). The five main SSPs Representative Climate Pathways (RCPs) combination used in CMIP6 are SSP1-2.6, SSP2-4.5, SSP3-7.0, SSP4-6.0, and SSP5-8.5 (Hausfather 2018). The full list of LOCA2-Hybrid climate model projections included in this analysis is presented in Table B-2.

Table B-2. List of Ensemble Members of the CMIP6 Downscaled Datasets

S. No.	Model	Experiment	Variant
1	ACCESS-CM2	SSP2-4.5	r1i1p1f1
2	ACCESS-CM2	SSP3-7.0	r1i1p1f1
3	ACCESS-CM2	SSP5-8.5	r1i1p1f1
4	CESM2-LENS	SSP3-7.0	r1i1p1f1
5	CNRM-ESM2-1	SSP2-4.5	r1i1p1f2
6	CNRM-ESM2-1	SSP3-7.0	r1i1p1f2
7	CNRM-ESM2-1	SSP5-8.5	r1i1p1f2
8	EC-Earth3	SSP2-4.5	r1i1p1f1
9	EC-Earth3	SSP3-7.0	r1i1p1f1
10	EC-Earth3	SSP5-8.5	r1i1p1f1
11	EC-Earth3-Veg	SSP2-4.5	r1i1p1f1
12	EC-Earth3-Veg	SSP3-7.0	r1i1p1f1

S. No.	Model	Experiment	Variant
13	EC-Earth3-Veg	SSP5-8.5	r1i1p1f1
14	FGOALS-g3	SSP2-4.5	r1i1p1f1
15	FGOALS-g3	SSP3-7.0	r1i1p1f1
16	FGOALS-g3	SSP5-8.5	r1i1p1f1
17	GFDL-ESM4	SSP2-4.5	r1i1p1f1
18	GFDL-ESM4	SSP3-7.0	r1i1p1f1
19	GFDL-ESM4	SSP5-8.5	r1i1p1f1
20	HadGEM3-GC31-LL	SSP2-4.5	r1i1p1f3
21	HadGEM3-GC31-LL	SSP5-8.5	r1i1p1f3
22	INM-CM5-0	SSP2-4.5	r1i1p1f1
23	INM-CM5-0	SSP3-7.0	r1i1p1f1
24	INM-CM5-0	SSP5-8.5	r1i1p1f1
25	IPSL-CM6A-LR	SSP2-4.5	r1i1p1f1
26	IPSL-CM6A-LR	SSP3-7.0	r1i1p1f1
27	IPSL-CM6A-LR	SSP5-8.5	r1i1p1f1
28	KACE-1-0-G	SSP2-4.5	r1i1p1f1
29	KACE-1-0-G	SSP3-7.0	r1i1p1f1
30	KACE-1-0-G	SSP5-8.5	r1i1p1f1
31	MIROC6	SSP2-4.5	r1i1p1f1
32	MIROC6	SSP3-7.0	r1i1p1f1
33	MIROC6	SSP5-8.5	r1i1p1f1
34	MPI-ESM1-2-HR	SSP2-4.5	r1i1p1f1
35	MPI-ESM1-2-HR	SSP3-7.0	r1i1p1f1
36	MPI-ESM1-2-HR	SSP5-8.5	r1i1p1f1
37	MRI-ESM2-0	SSP2-4.5	r1i1p1f1
38	MRI-ESM2-0	SSP3-7.0	r1i1p1f1
39	MRI-ESM2-0	SSP5-8.5	r1i1p1f1
40	TaiESM1	SSP2-4.5	r1i1p1f1
41	TaiESM1	SSP3-7.0	r1i1p1f1

The associated changes in temperature, precipitation, extreme heat days, and extreme precipitation were compared between the Coupled Model Intercomparison Project Phase 5 (CMIP5) and Phase 6 (CMIP6) datasets. Twenty individual downscaled general circulation model (GCM) projections were selected from 10 different CMIP5 GCMs and 2 different RCPs, RCP 4.5 and RCP 8.5. These 20 climate projections were downscaled using the LOCA statistical downscaling method at 1/16th degree (~6 km or ~3.75 miles) spatial resolution by Scripps Institution of Oceanography (Pierce et al. 2014). The summary of key differences between CMIP5 and CMIP6 results over the Russian River watershed is available in Attachment 1.

B.3.1 Basin Characterization Model

The BCM was developed by the US Geological Survey (USGS) and serves as a regional water balance model that simulates historical and future climate unimpaired streamflows and evapotranspiration (Flint et al. 2021). BCMs have been developed for several areas across California; the initial development of the Russian River and Upper Eel River BCM was completed in 2009. Since then, the local BCM has been updated several times, with the most recent update in 2025 adding Marin County reservoirs. To date, the BCM has been used in several Russian River water supply planning studies, including the *Lake Mendocino Water Supply Reliability Evaluation Report* (Sonoma Water 2017), *Fish Habitat Flow and Water Rights Project Draft EIR* (Sonoma Water 2016), and *Sonoma Water Climate Adaptation Plan* (Sonoma Water 2021).

The BCM simulates unimpaired hydrologic conditions by balancing precipitation, evapotranspiration, sublimation, runoff, recharge, and soil-moisture change at each grid cell. Excess water infiltrates only when precipitation exceeds potential evapotranspiration, with recharge representing percolation below the evaporative zone and saturation leading to runoff. Spatial patterns of recharge and runoff reflect local climate, land cover, and subsurface properties. Model inputs include solar radiation, potential evapotranspiration, precipitation, and air temperature, using PRISM for historical data and LOCA2-Hybrid downscaled GCMs for future projections. Outputs include sublimation, snow processes, excess water, local recharge and runoff, actual evapotranspiration, climatic water deficit, and processed basin discharge and groundwater estimates. The BCM model simulations were conducted at a daily time step and 270-meter spatial resolution for the Russian River and Upper Eel River from 1910 to 2024, and for the Marin reservoirs from 1981 to 2024. The future simulations were performed for 2015–2100 using the CMIP6 LOCA2-Hybrid downscaled climate dataset. Future land use assumptions were not represented in simulations of future conditions in the BCM modeling. More details on the BCM model are available at https://pubs.usgs.gov/tm/06/h01/tm6h1.pdf.

B.3.2 Climate Vulnerability Assessment

B.3.2.1 Temperature

Climate change is expected to cause an increase in temperature in the future. Projected changes in temperature are calculated by analyzing the following index:

- *Projected changes in average annual temperature*

Methodology: Temperature metric is estimated using the projected temperature from 15 climate models under SSP2-4.5 (Shared Socioeconomic Pathway), SSP3-7.0, and SSP5-8.5. Projected temperature from 41 climate projections is used to estimate the change in annual temperature. The median changes are calculated for mid future (2041-2070) and late future (2071-2100) periods with respect to historical period (1981-2010).

Approach

a. Daily average temperature for the 270 m grids in Russian River watershed domain was used from the 41 climate projections. The 270 m dataset was generated through the spatial interpolation of the original LOCA2-Hybrid dataset, which is provided at a1/32° grid resolution.

b. The daily temperature was accumulated at annual scale (October to September) for estimating the index values during historical (1981 to 2010), mid (2041 to 2070), and late (2071 to 2100) future periods.

c. The absolute values of the annual index during the historical, mid, and late future periods were utilized to calculate the relative change for the future periods for 41 climate projections.

d. The projected change in the temperature was reported as the median change of the annual index from the 41 climate projections during the mid and late future.

Key Results: The annual average temperature is projected to increase by 3.7°F during the mid future and 6°F during the late future as compared to the historical reference value of 57°F (Figure B-6). Future climate projections for the Russian River region indicate a substantial and consistent rise in average temperatures. This warming trend is evident across all climate projections, though the magnitude varies by climate model projection. Higher temperatures are expected to directly affect multiple resource sectors, including surface water supply, groundwater, and ecosystems, by intensifying evaporation, increasing water demand, and raising water temperatures.

Figure B-6. Change in the Annual Temperature During Mid Future (2041 to 2070, center, °F) and Late Future (2071 to 2100, right, °F) with Respect to Historical Period (1981 to 2010, left, °F) Using 270 m Interpolated Data from 15 CMIP6 Climate Models under SSP2-4.5, SSP3-7.0, and SSP5-8.5

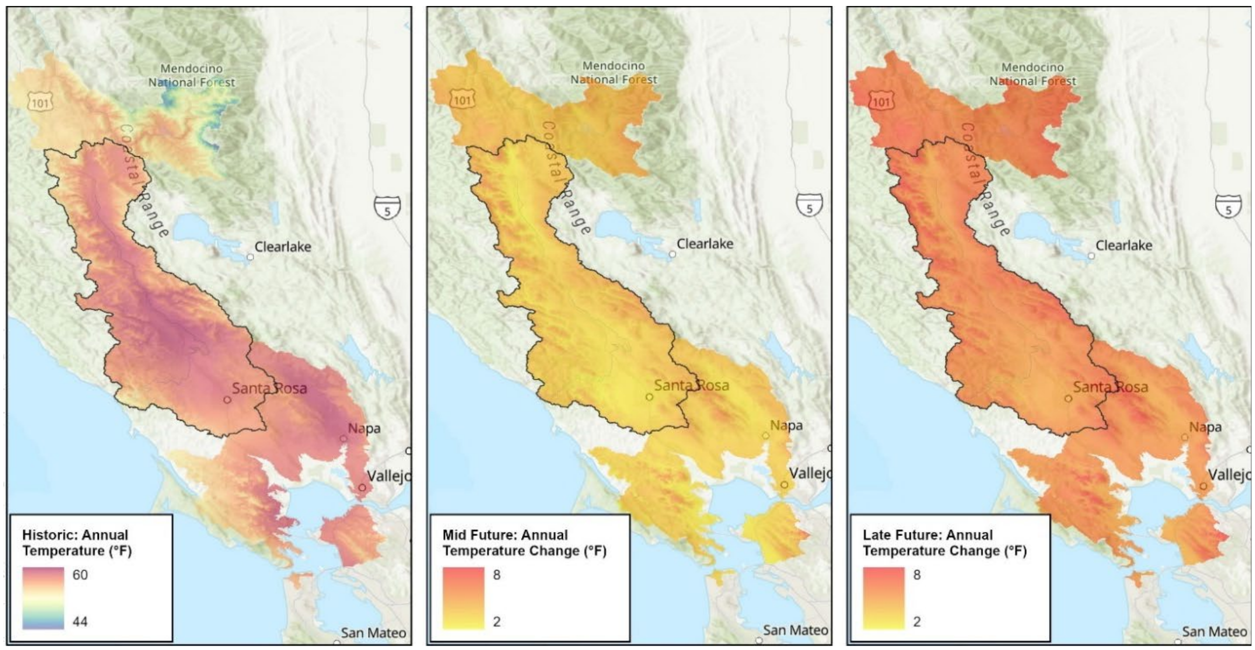

B.3.2.2 Extreme Heat Days

Climate change is expected to cause an increase in heat days due to rise in temperature in the future. Projected changes in heat days are calculated by analyzing the following index:

- *Projected changes in extreme heat days*

Methodology: Extreme Heat Days metric is estimated using the projected temperature from 15 climate models under SSP2-4.5 (Shared Socioeconomic Pathway), SSP3-7.0, and SSP5-8.5. Projected maximum temperature from 41 climate projections is used to estimate the change in extreme heat days. Extreme heat days are defined as the days of the year when daily maximum temperature is above 95°F. The median changes are calculated for mid future (2041-2070) and late future (2071-2100) periods with respect to historical period (1981-2010).

Approach

a. Daily maximum temperature for the 270 m grids in Russian River watershed domain was used from the 41 climate projections. The 270 m dataset was generated through the spatial interpolation of the original LOCA2-Hybrid dataset, which is provided at a1/32° grid resolution. Daily extreme heat day was identified as days with maximum temperature higher than 95°F.

b. The daily extreme heat days were accumulated at annual scale (October to September) for estimating the index values during historical (1981 to 2010), mid (2041 to 2070), and late (2071 to 2100) future periods.

c. The absolute values of the annual index during the historical, mid, and late future periods were utilized to calculate the absolute change for the future periods for 41 climate projections.

d. The projected change in the extreme heat days was reported as the median change of the annual index from the 41 climate projections during the mid and late future.

Key Results: The extreme heat days are projected to increase by 17 days/year during the mid future and 32 days/year during the late future as compared to the historical reference value of 15 days/year (Figure B-7). These increases are not uniform, with the central and northern portions of the watershed experiencing the greatest intensification. Warmer stream and river temperatures will reduce suitable habitat for cold-water species. Expanded exposure to extreme heat may significantly affect multiple water-resource-related sectors, including recreation, ecosystem health, surface water supply, and hydropower, by elevating temperature-driven stress on natural systems, infrastructure, and human use patterns.

Figure B-7. Change in the Extreme Heat Days During Mid Future (2041 to 2070, center, days/year) and Late Future (2071 to 2100, right, days/year) with Respect to Historical Period (1981 to 2010, left, days/year) Using 270 m Interpolated Data from 15 CMIP6 Climate Models under SSP2-4.5, SSP3-7.0, and SSP5-8.5

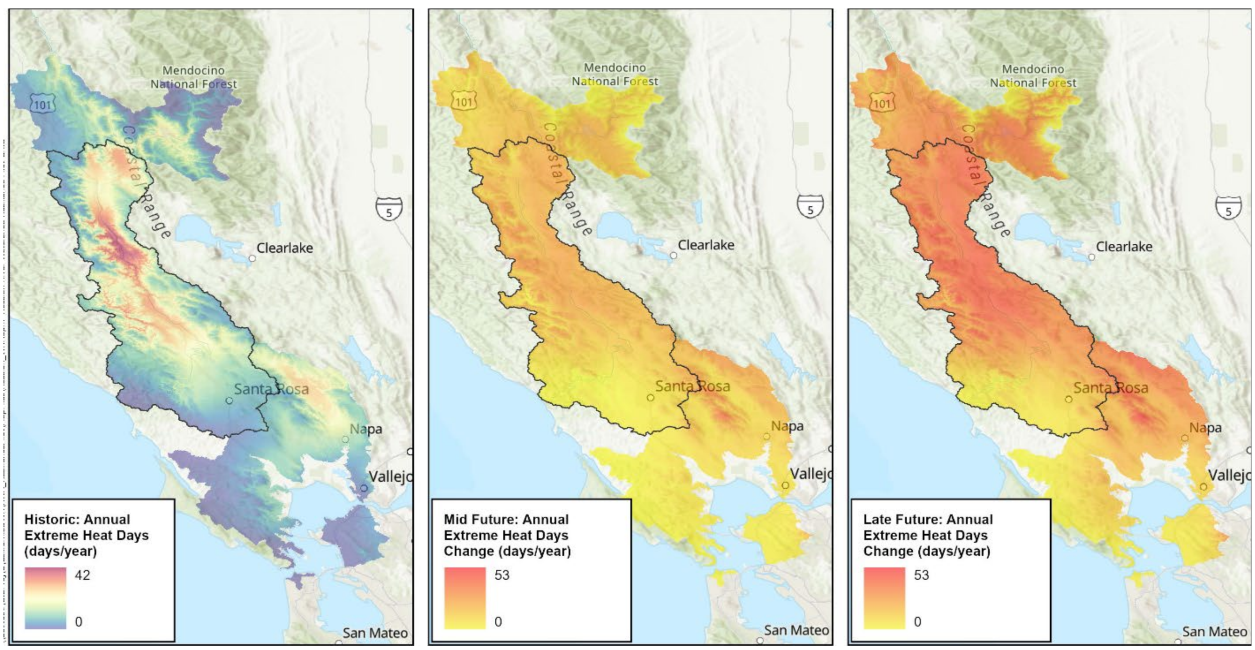

B.3.2.3 Precipitation

Climate change is expected to change the average precipitation in the future. Projected changes in precipitation are calculated by analyzing the following index:

- *Projected changes in average annual precipitation*

Methodology: Precipitation metric is estimated using the projected precipitation from 15 climate models under SSP2-4.5 (Shared Socioeconomic Pathway), SSP3-7.0, and SSP5-8.5. Projected precipitation from 41 climate projections is used to estimate the change in annual precipitation. The median changes are calculated for mid future (2041–2070) and late future (2071–2100) periods with respect to historical period (1981–2010).

Approach

a. Daily precipitation for the 270 m grids in Russian River watershed domain was used from the 41 climate projections. The 270 m dataset was generated through the spatial interpolation of the original LOCA2-Hybrid dataset, which is provided at a1/32° grid resolution.

b. The daily precipitation was accumulated at annual scale (October to September) for estimating the index values during historical (1981 to 2010), mid (2041 to 2070), and late (2071 to 2100) future periods.

c. The absolute values of the annual index during the historical, mid, and late future periods were utilized to calculate the relative change for the future periods for 41 climate projections.

d. The projected change in the precipitation was reported as the median change of the annual index from the 41 climate projections during the mid and late future.

Key Results: The annual precipitation is projected to increase by 2.9% during the mid future and 5% during the late future as compared to the historical reference value of 43 inches (Figure B-8). Climate projections for most of the Russian River region indicate a modest but consistent increase in annual precipitation across future time periods. While the overall regional trend suggests wetter conditions, localized areas may experience declines in precipitation, highlighting spatial variability in climate responses. These changes have implications for several water-resource sectors, including surface water supply, groundwater recharge, hydropower production, and ecosystem health, each of which is sensitive to long-term precipitation patterns.

Figure B-8. Change in the Annual Precipitation During Mid Future (2041 to 2070, center, %) and Late Future (2071 to 2100, right, %) with Respect to Historical Period (1981 to 2010, left, inch) Using 270 m Interpolated Data from 15 CMIP6 Climate Models under SSP2-4.5, SSP3-7.0, and SSP5-8.5

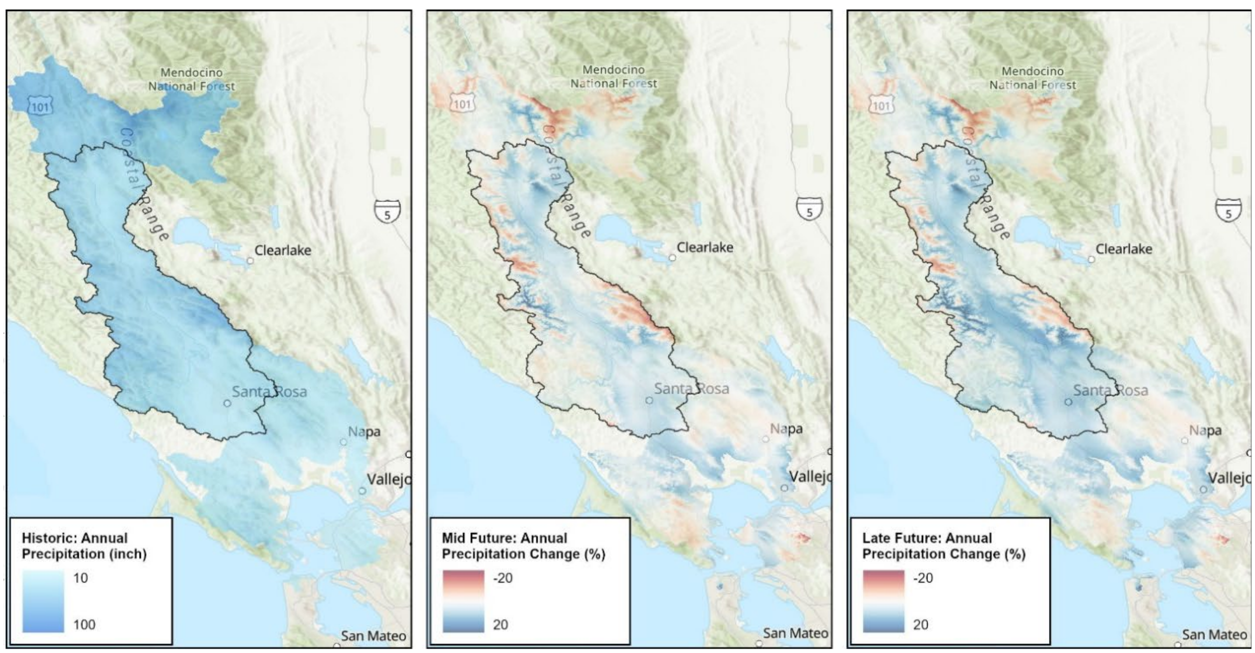

B.3.2.4 Extreme Precipitation

Climate change is expected to change the extreme precipitation in the future. The projected changes in 1% annual exceedance probability (AEP) value are calculated based on daily precipitation in the future periods compared to historical period. Projected changes in extreme precipitation are calculated by analyzing the following index:

- *Projected changes in extreme precipitation*

Methodology: Extreme precipitation metric is estimated using the projected precipitation from 15 climate models under SSP2-4.5 (Shared Socioeconomic Pathway), SSP3-7.0, and SSP5-8.5. Projected precipitation from 41 climate projections is used to estimate the change in extreme precipitation. Extreme precipitation is defined as the 1% AEP precipitation value. The maximum value is estimated for each water year from daily precipitation time series. The change in the 99^{th} percentile values of the daily maxima precipitation is computed for mid future (2041-2070) and late future (2071-2100) periods with respect to historical period (1981-2010) and the median from the 41 climate projections is estimated.

Approach

a. Daily precipitation for the 270 m grids in Russian River watershed domain was used from the 41 climate projections. The 270 m dataset was generated through the spatial interpolation of the original LOCA2-Hybrid dataset, which is provided at a1/32° grid resolution.

b. The daily precipitation was utilized for estimating 99^{th} percentile values of daily maxima precipitation for each water year at annual scale (October to September) for estimating the index values during historical (1981 to 2010), mid (2041 to 2070), and late (2071 to 2100) future periods.

c. The absolute values of the annual index during the historical, mid, and late future periods were utilized to calculate the relative change for the future periods for 41 climate projections.

d. The projected change in the extreme precipitation was reported as the median change of the annual index from the 41 climate projections during the mid and late future.

Key Results: The extreme precipitation is projected to increase by 6% during the mid future and 17% during the late future as compared to the historical reference value of 6 inches (Figure B-9). Future climate projections show a notable increase in extreme precipitation across the Russian River region. Spatial variability mirrors overall precipitation patterns, with the southern portion of the watershed showing the most pronounced increases. The projected intensification of extreme precipitation events is a primary driver of increased flood risk under future climate conditions. These changes are expected to affect multiple water resource sectors, including flood management, groundwater recharge, and surface water supply.

Figure B-9. Change in the Extreme Precipitation During Mid Future (2041 to 2070, center, %) and Late Future (2071 to 2100, right, %) with Respect to Historical Period (1981 to 2010, left, inch) Using 270 m Interpolated Data from 15 CMIP6 Climate Models under SSP2-4.5, SSP3-7.0, and SSP5-8.5

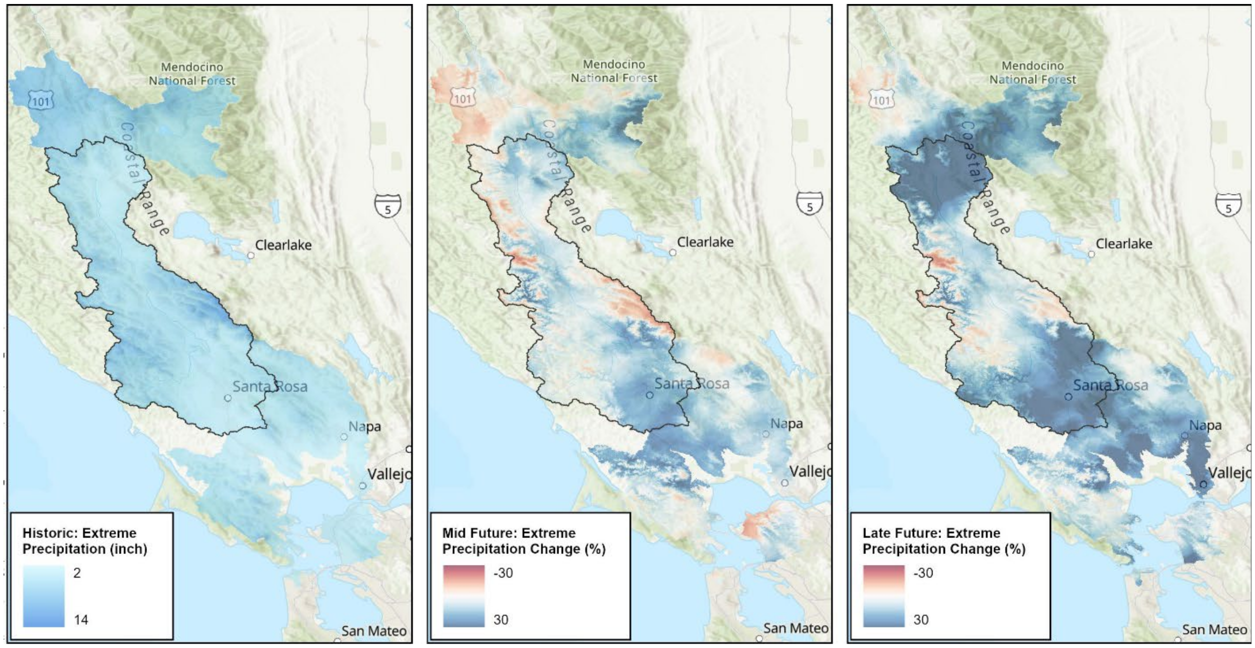

B.3.2.5 Sea Level Rise

Sea levels in the Pacific Ocean influence conditions in the lower Russian River watershed, altering the hydrology of the Russian River Estuary and the quantity of suitable habitat for aquatic species in this area. Since 1975, the Russian River watershed (measured at Point Reyes) has experienced 0.35 feet of sea level rise (NOAA 2026). Melting ice sheets and glaciers as well as the thermal expansion of seawater associated with increased global temperatures are the primary causes for increase in global mean sea levels in the past century. Development of sea level rise projections is typically performed by incorporating SSPs to model the physical processes associated with sea level rise. The Pilot leverages sea level projections identified by the California Ocean Protection Council's *State of California Sea-Level Rise Guidance 2024 Science and Policy Update* for evaluation of ecosystem vulnerabilities in the Russian River Estuary. Under future conditions, the Russian River watershed (modeled at Point Reyes) could experience further rise in sea level of between 0.8 to 1.3 feet by 2050, and 3.1 to 6.6 feet by 2100 (California Ocean Protection Council 2024). Additional details on sea level rise assumptions utilized for this effort are provided in Appendix C.

B.3.3 Hydrological Vulnerability Assessment

B.3.3.1 Runoff

Climate change is expected to change the total runoff in the future. Projected changes in runoff are calculated by analyzing the following index:

- *Projected changes in average total runoff*

Methodology: BCM model-simulated runoff and recharge fluxes for 15 climate models under SSP2-4.5, SSP3-7.0, and SSP5-8.5 are used to estimate the change in annual total runoff. Total runoff is defined as the grid-based flow using the summation of runoff and recharge aggregated at the annual scale based on each water year. The median changes are calculated for mid future (2041–2070) and late future (2071-2100) periods with respect to historical period (1981-2010).

Approach

a. BCM model-simulated daily total runoff for the 270 m grids in Russian River watershed domain was estimated by grid-wise summation of the runoff and recharge from the 41 climate projections. BCM simulated runoff and recharge values are all the grids that were extracted separately for the different climate projections.

b. The daily total runoff was accumulated at annual scale (October to September) for estimating the index values during historical (1981 to 2010), mid (2041 to 2070), and late (2071 to 2100) future periods.

c. The absolute values of the annual index during the historical, mid, and late future periods were utilized to calculate the relative change for the future periods for 41 climate projections.

d. The projected change in the total runoff was reported as the median change of the annual index from the 41 climate projections during the mid and late future.

Key Results: The annual total runoff is projected to decrease by 1% during the mid future and increase 2% in the late future as compared to the historical reference value (Figure B-10). Model results indicate that while annual total runoff across most of the Russian River watershed is expected to decline slightly in the mid-future period, it is anticipated to rise again under late-future climate conditions. Spatial patterns of change closely mirror those projected for precipitation, with some areas experiencing greater increases than others. While elevated runoff may offer potential benefits for surface water supply, hydropower, recreation, groundwater recharge, and agricultural water availability, the increased variability also heightens the risk of drought in years where runoff declines.

Figure B-10. Change in the Total Runoff During Mid Future (2041 to 2070, center, %) and Late Future (2071 to 2100, right, %) with Respect to Historical Period (1981 to 2010, left, TAF) Using 270 m Interpolated Data from 15 CMIP6 Climate Models under SSP2-4.5, SSP3-7.0, and SSP5-8.5

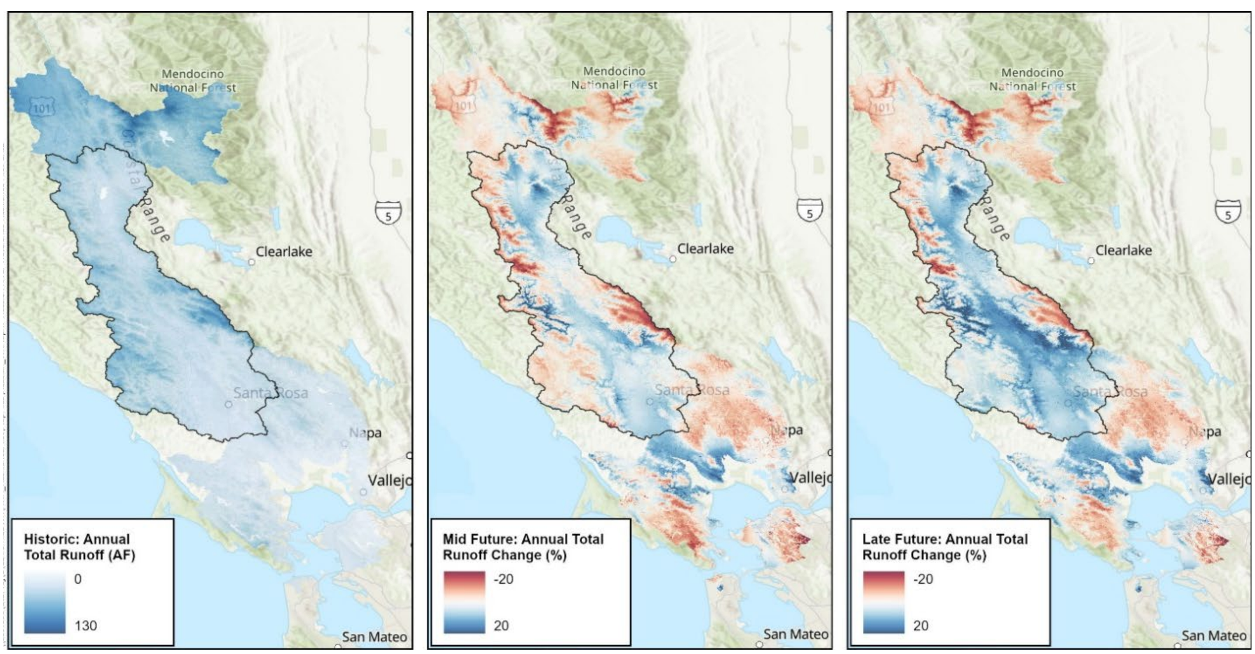

B.3.3.2 Floods

Flood impacts are estimated by forecasting the impacts of flood events for the future period. The projected changes in 1% AEP flows are calculated based on 1-day and 3-day unimpaired flow in future period compared to historical period. Projected changes in floods are calculated by analyzing the following indices:

- *Projected changes in 1% AEP flows based on 1-day unimpaired flow*
- *Projected changes in 1% AEP flows based on 3-day unimpaired flow*

Methodology: Flood analysis is conducted using the BCM model-simulated total runoff (summation of runoff and recharge) for 15 climate models under SSP2-4.5, SSP3-7.0, and SSP5-8.5. Total runoff is defined as the grid-based flow using the summation of runoff and recharge. A 1-day and 3-day moving average for total runoff is generated from daily fluxes and the maximum value is estimated for the water years. The change in the 99th percentile values of the 1-day and 3-day maxima total runoff is computed for mid future (2016 to 2065) and late future (2051 to 2100) periods with respect to historical period (1961 to 2010) and the median from the 41 climate projections is estimated.

Approach

a. BCM model-simulated daily total runoff for the 270 m grids in Russian River watershed domain was estimated by grid-wise summation of the runoff and recharge from the 41 climate projections. BCM simulated runoff and recharge values are all the grids that were extracted separately for the different climate projections.

b. For 1-day exceedance probability, the daily total runoff was utilized for estimating the annual maxima of daily total runoff for estimating the 99th percentile values during historical (1981 to 2010), mid (2041 to 2070), and late (2071 to 2100) future periods. For 3-day exceedance probability, the 3-day moving average total runoff was estimated from the daily total runoff and the 99th percentile values were estimated based on annual maxima 3-day total runoff for historical, mid, and late future periods.

c. The absolute values of the 99th percentile values of the daily maxima and 3-day maxima total runoff during the historical, mid, and late future periods were utilized to calculate the relative change for the future periods for 41 climate projections.

d. The projected change in the flood was reported as the median change of the index from the 41 climate projections during the mid and late future.

Key Results: The 1-day flood magnitude is projected to increase by 1% in the mid-future period and by 8.6% in the late-future period (Figure B-11). In comparison, the projected increase in the 3-day flood is slightly lower, with estimated changes of 3.5% for the mid-future and 8.1% for the late-future period (Figure B-12). Projected changes indicate that, although 1-day and 3-day flood flows generally increase across the Russian River watershed, several sub-regions exhibit decreases in these flood metrics during both the mid-future and late-future periods. Spatial patterns of change resemble those of extreme precipitation, with the most pronounced increases occurring in the southern portion of the watershed. These increases have implications for surface water supply operations, recreation, flood management infrastructure, and ecosystem function.

Figure B-11. Change in the 1-day flood During Mid Future (2016 to 2065, center, %) and Late Future (2051 to 2100, right, %) with Respect to Historical Period (1961 to 2010, left, TAF) Using 270 m Interpolated Data from 15 CMIP6 Climate Models under SSP2-4.5, SSP3-7.0, and SSP5-8.5

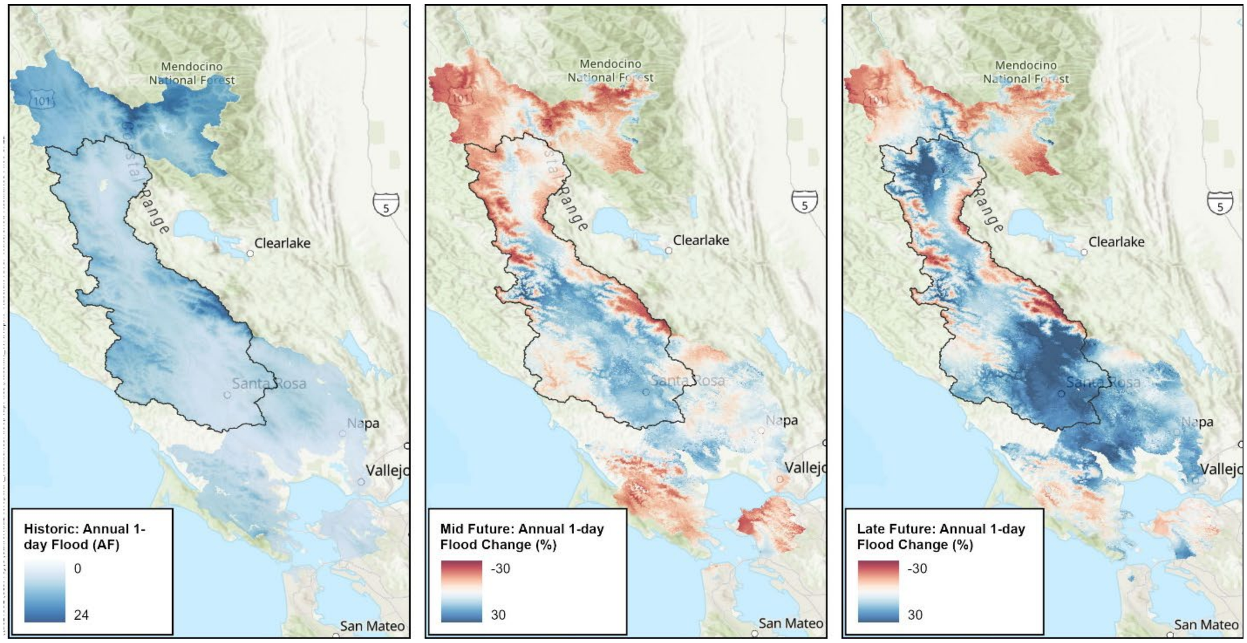

Figure B-12. Change in the 3-day Flood During Mid Future (2016 to 2065, center, %) and Late Future (2051 to 2100, right, %) with Respect to Historical Period (1961 to 2010, left, TAF) Using 270 m Interpolated Data from 15 CMIP6 Climate Models under SSP2-4.5, SSP3-7.0, and SSP5-8.5

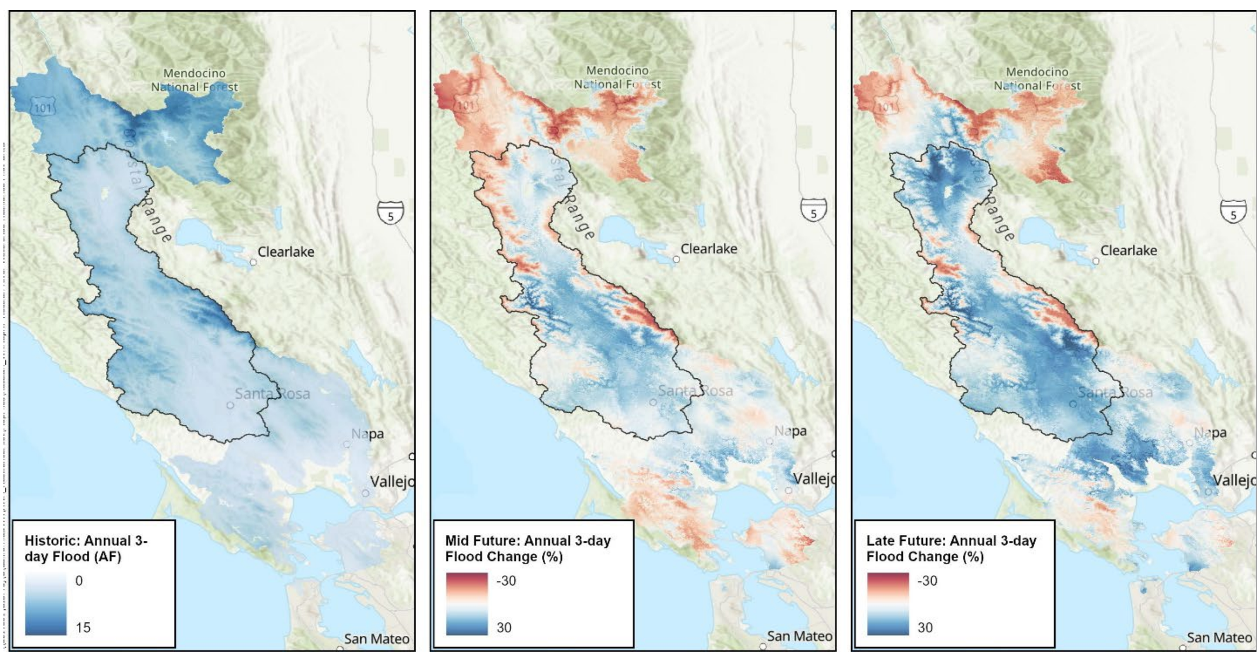

B.3.3.3 Drought

Drought is assessed by comparing the projected water deficit conditions for future climate conditions. Projected changes in drought are calculated by analyzing the following index:

- *Projected changes in drought severity*

Methodology: BCM model-simulated runoff and recharge fluxes models for 15 climate models under SSP2-4.5, SSP3-7.0, and SSP5-8.5 are used to estimate the change in drought severity. Total runoff is defined as the grid-based flow using the summation of runoff and recharge aggregated at the annual scale based on each water year.

Drought severity is estimated using the grid-based runoff deficit simulated by the BCM model for 41 climate projections. Although there are many different categories of drought (meteorological, hydrological, agricultural, and socioeconomic), and approaches to measuring drought (Standardized precipitation index, Palmer drought severity index, surface water supply index), for the purpose of this assessment, drought is calculated as the annual change in the dryness (runoff). This method is chosen for its simplicity and consistency across all watersheds. Drought severity is defined as the maximum summation of the consecutive negative values. The change in the index is estimated as the median change from 41 climate projections for mid future (2016 to 2065) and late future (2051 to 2100) periods with respect to historical period (1961 to 2010).

Approach

a. BCM model-simulated daily total runoff for the 270 m grids in Russian River watershed domain was estimated by grid-wise summation of the runoff and recharge from the 41 climate projections. BCM simulated runoff and recharge values are all the grids that were extracted separately for the different climate projections.

b. The daily values were accumulated at annual water-year scale for the estimation of the historical annual mean for historical (1961 to 2010), mid (2016 to 2065), and late (2051 to 2100) future periods. Runoff deficit (when annual value minus long-term historical value is negative) was calculated for each year for mid and late future periods using the historical annual value as threshold.

c. The years with the positive deficit value were assigned to be zero. The cumulative deficit values were estimated for the consecutive negative values. The drought severity was estimated as the minimum value of the cumulative annual deficit value for the historical, mid, and late future periods.

d. The relative percentage change in the drought severity was calculated for the historical, near, and late future periods from 41 climate projections.

e. The projected change in drought severity was reported as the median change of the annual index from the 41 climate projections during the mid and late future.

Key Results: The drought severity is projected to increase by 5.5% during the mid future and 5.4% during the late future (Figure B-13). Future climate projections indicate a measurable increase in drought severity across the Russian River region. The primary drivers of this increase include rising temperatures and localized reductions in runoff, which collectively intensify drying conditions across much of the watershed. These changes elevate risks to water supply reliability, ecosystem health, and agricultural productivity, with severe drought conditions also contributing to heightened wildfire risk.

Figure B-13. Change in the Drought Severity During Mid Future (2016 to 2065, center, %) and Late Future (2051 to 2100, right, %) with Respect to Historical Period (1961 to 2010, left, TAF) Using 270 m Interpolated Data from 15 CMIP6 Climate Models under SSP2-4.5, SSP3-7.0, and SSP5-8.5

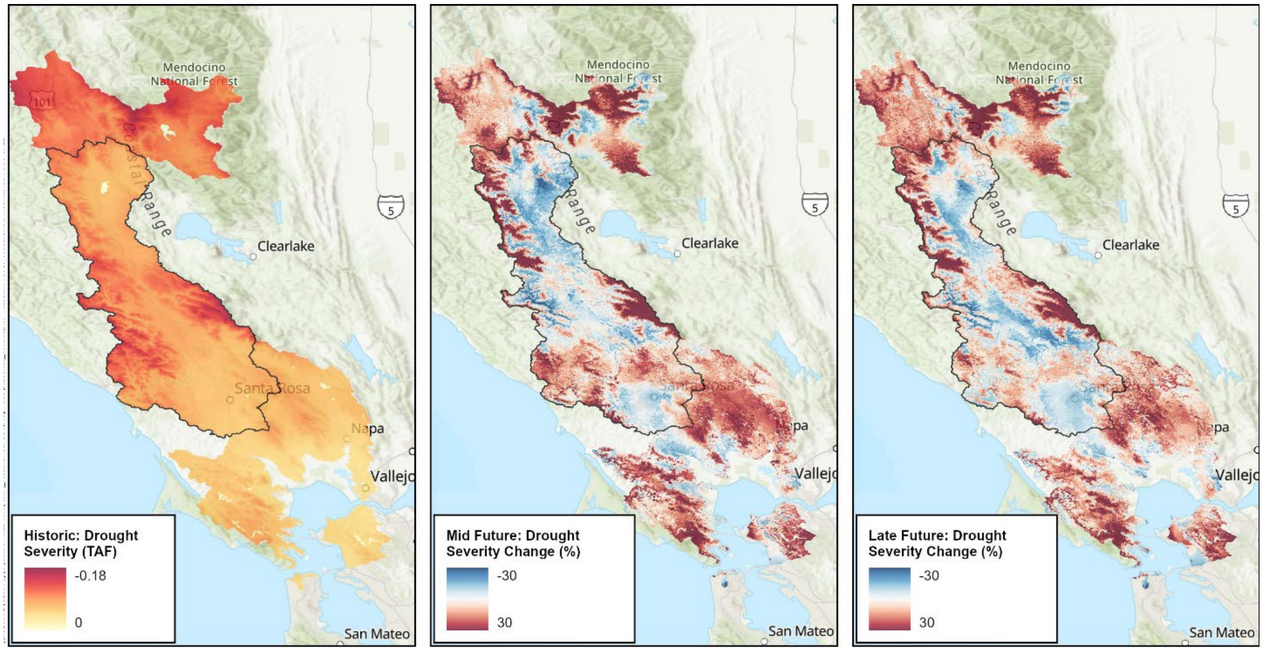

Figure B-14 shows the total flow at Healdsburg for Paleo-reconstruction records (1582–2004), historical period (1911–2025), and future projections using CMIP6 climate models (2026–2100). Paleo-reconstructed flows at Healdsburg show large natural variability, with repeated multi-decadal wet and dry periods but a long-term average broadly similar to the modern historical record. The instrumental period captures this variability with more precise measurements and highlights several extreme droughts and floods. Future projections indicate continued high year-to-year variability, with a wider spread between very wet and very dry years, suggesting increased hydrologic volatility under changing climate conditions. The total flow at Healdsburg shows both consistency in long-term averages and substantial variability across the paleo, historical, and projected future periods (Figure B-15). The paleo-reconstruction period exhibits a median flow of about 897 TAF, with a wide range from 0 to 2,188 TAF, reflecting natural climate variability and episodes of both severe drought and major flood years. The instrumental historical period shows a similar central tendency, with a median of 872 TAF and a range from 45 to 2,233 TAF, but with tighter bounds and more precise measurement, capturing several notable hydrologic extremes. Future projections indicate that median flows remain comparable at roughly 876 TAF, but the range widens significantly, from as low as 1 TAF to as high as 2,869 TAF, suggesting increased hydrological volatility and the potential for more frequent extreme wet and dry years under future climate conditions.

Figure B-14. The Total Flow at Healdsburg for Paleo-reconstruction Records (1582–2004), Historical Period (1911–2025), and Future Projections (2026–2100)

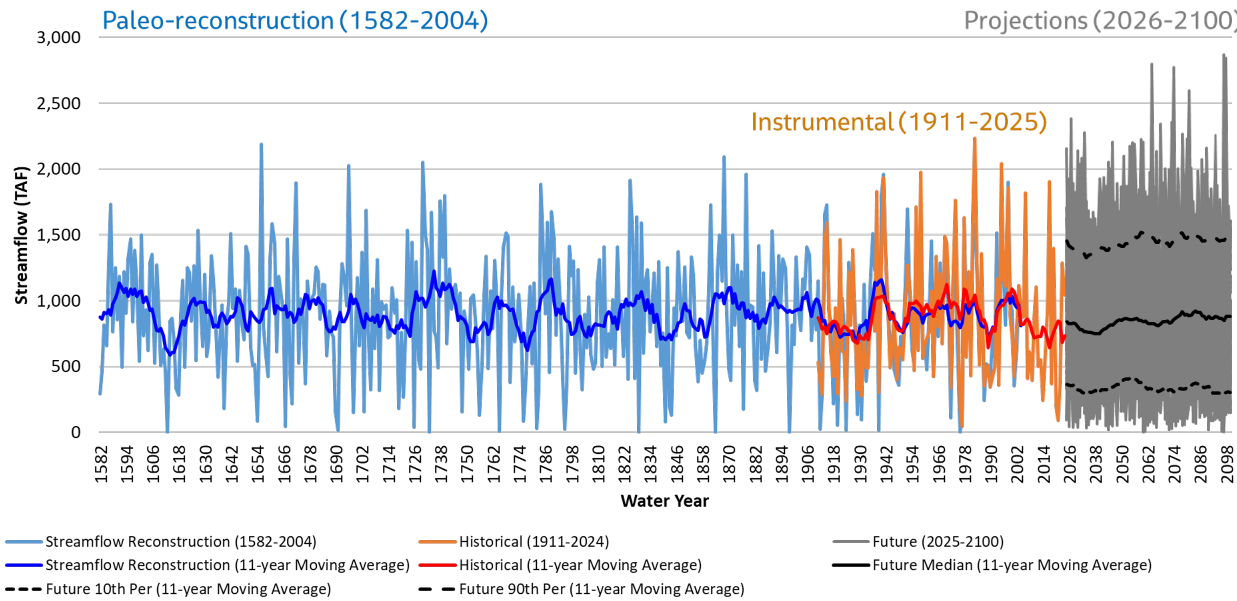

Figure B-15. Statistics of the Total Flow at Healdsburg for Paleo-reconstruction Records (1582–2004), Historical Period (1911–2025), and Future Projections (2026–2100)

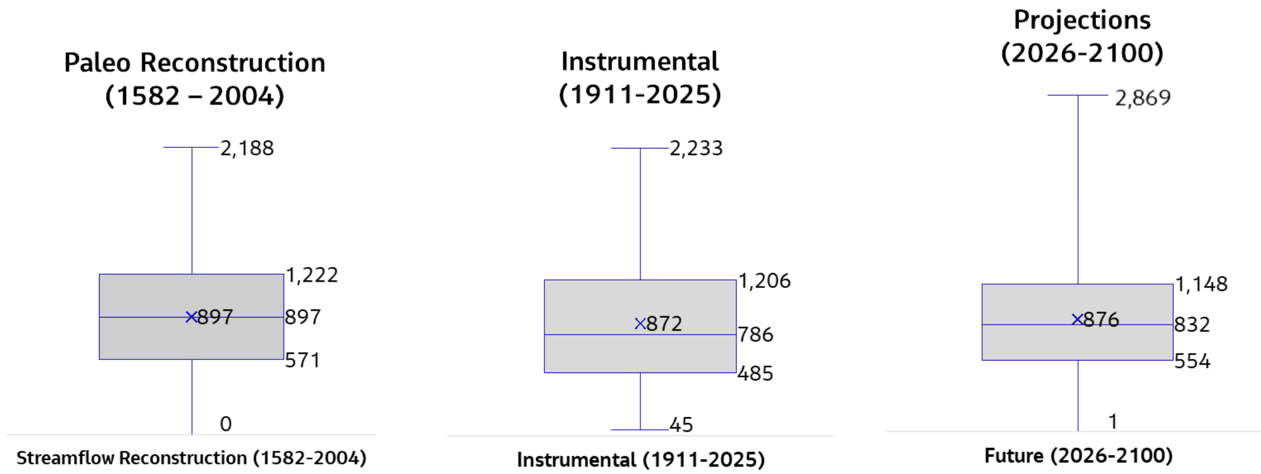

Drought severity and duration were also estimated using the inflow to Healdsburg for paleo data (1582–2025), observed data (1941–2025), and 41 climate projections (Figures 16 to 18). Streamflow deficit (when annual value minus long-term historical value is negative) was calculated for each year using the historical annual value as threshold. The years with the positive deficit value were assigned to be zero. The cumulative deficit values and number of years were estimated for the consecutive negative values. The drought severity was estimated as the minimum value of the cumulative annual deficit value and the drought duration was estimated as the maximum values of the cumulative years with streamflow deficit.

Paleo-hydrologic reconstructions reveal that the Russian River basin has historically experienced droughts of both greater duration and magnitude than those captured in the instrumental record. While the 1976–77 and 2020–22 droughts remain among the most severe short-duration droughts, the paleo record highlights longer multi-decadal drought episodes, most notably the prolonged drought of

1610–1619, indicating that the watershed is climatically predisposed to extended dry periods. These reconstructed patterns broaden the understanding of natural variability and provide context for assessing future drought risk under climate change.

Historical drought analysis also shows that the Russian River region has experienced significant variability in drought severity and duration over the period of record. The drought severity curves illustrate several notable multi-year drought events, with particular emphasis on the extreme short-duration droughts of 1987–92 and 2020–22. These events represent some of the most severe short-term deficits in observed history, characterized by rapid onset, sharp reductions in runoff, and sustained hydrologic stress.
The longest drought in the historical period was observed during 1943–50.

Future climate projections indicate an increase in both the severity and duration of droughts in the Russian River region. The analysis results show that future droughts are expected to exceed historical events in terms of cumulative deficit, length, and frequency, with more sustained multi-year droughts becoming increasingly common. These projected changes reflect the combined influence of higher temperatures, altered precipitation patterns, and earlier seasonal drying. The findings underscore increasing vulnerability of water supply, ecosystems, and hydrologic reliability as drought conditions intensify over the 21st century.

Figure B-16. Drought Severity and Duration Estimated Using the Natural Flows at Healdsburg for Paleo-reconstruction Period (1582–2025)

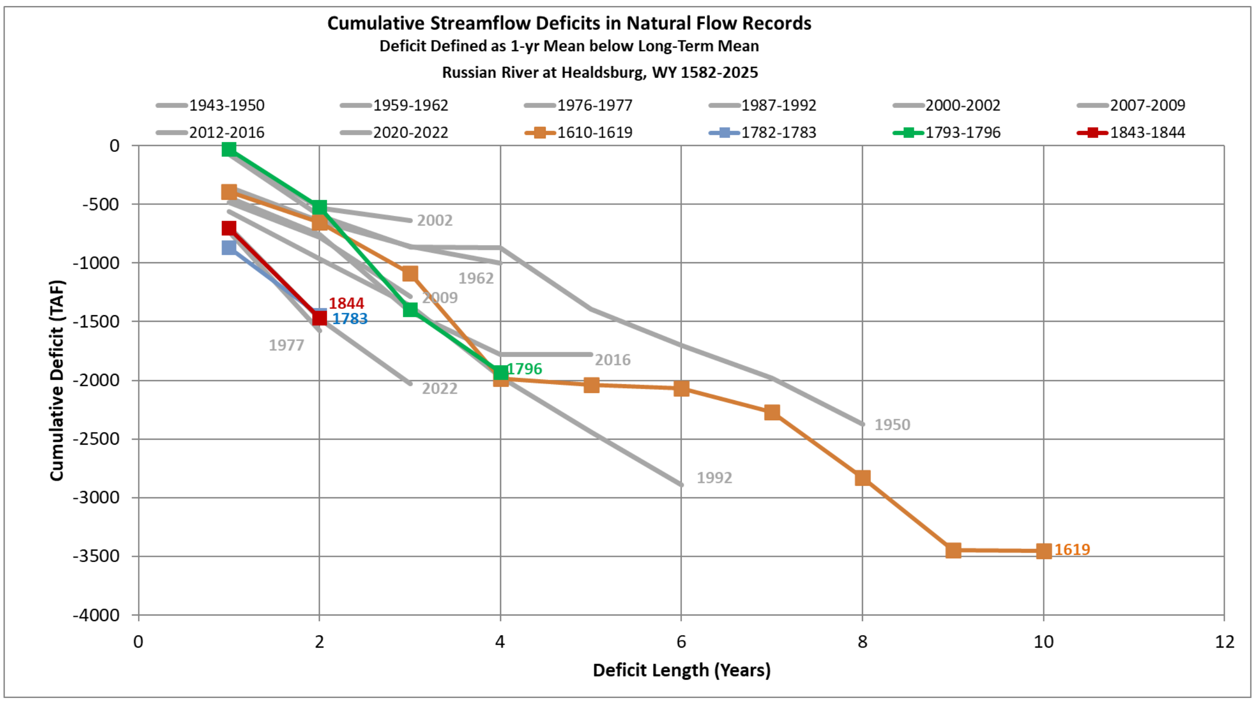

Figure B-17. Drought Severity and Duration Estimated Using the Natural Flows at Healdsburg for Observed Historical Period (1941–2025)

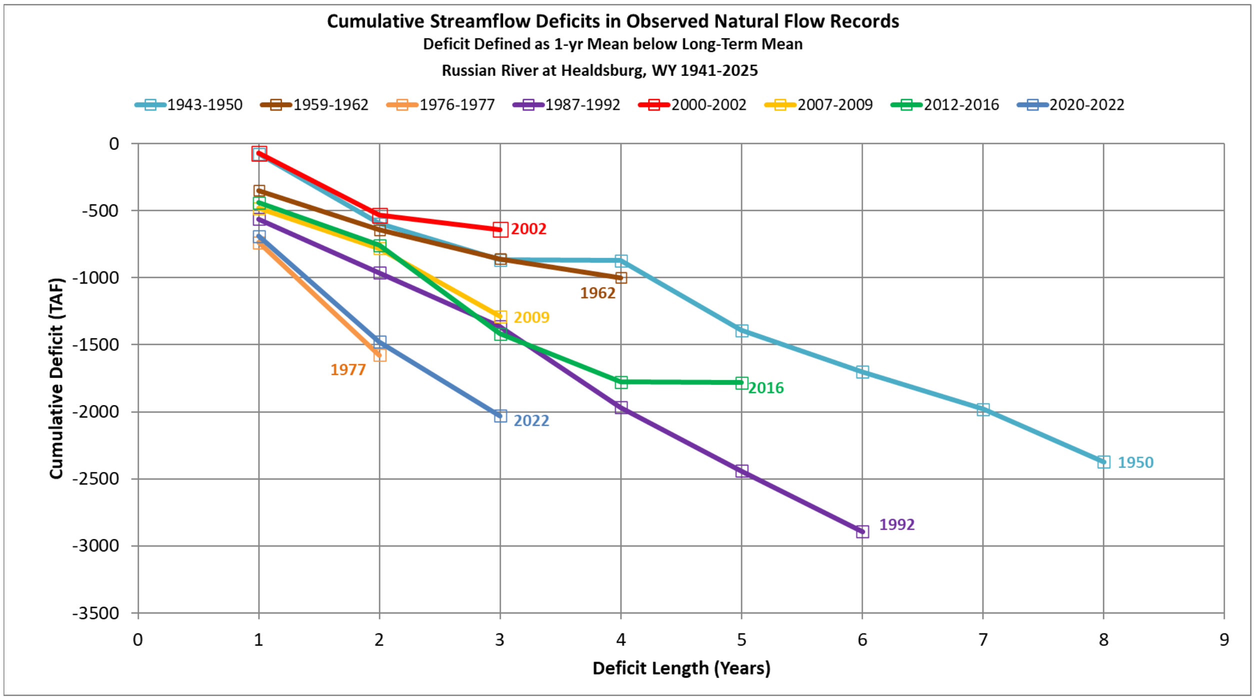

Figure B-18. Drought Severity and Duration Estimated Using the Natural Flows at Healdsburg for Future Period (1941–2100)

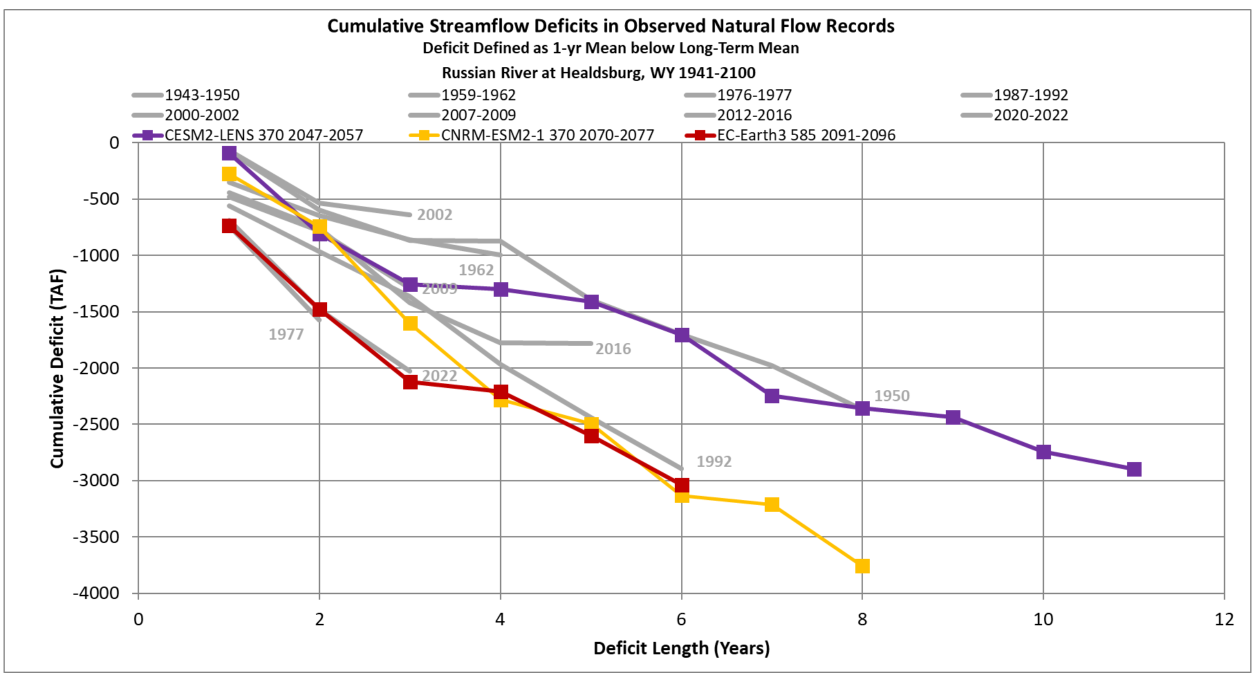

B.3.3.4 Wildfire

Increases in hot, dry weather can increase wildfire risk. Climate change can increase drought risks while higher temperatures create ideal conditions for fires to start and spread. Projected changes in wildfires are calculated by analyzing the following index:

- *Projected changes in decadal wildfire probabilities*

Methodology: Wildfire index is estimated using the decadal wildfire probability data for Business as Usual (BAU) population scenario and four climate models under RCP 4.5 and RCP 8.5 for CMIP5 from the Cal-Adapt database. The decadal wildfire probabilities median values are calculated for historical (1981 to 2010), mid future (2041 to 2070), and late future (2071 to 2100) periods. Decadal wildfire probability is representative of the probability that one or more fires occur in a given grid cell during a given decade.

Approach

a. Decadal wildfire probabilities data for BAU population scenario from four climate models under RCP 4.5 and RCP 8.5 for the 1/16th LOCA grids in Russian River watershed domain was accessed from the Cal-Adapt database.

b. The absolute values of the decadal wildfire probabilities were estimated for historical (1981 to 2010), mid future (2041 to 2070), and late future (2071 to 2100) periods for eight climate projections.

c. The projected values of the decadal wildfire probabilities were reported as the median change from the eight climate projections during the mid and late future under BAU population scenario.

Key Results: The average decadal wildfire probability for the region is 13% for the historical period and projected to be 18% for the mid future and 22% for the late future (Figure B-19). Wildfire probability is projected to increase substantially under future climate scenarios as drought conditions intensify, particularly across the northern and central parts of the watershed. The elevated risk is expected to worsen water quality, stress ecosystems, reduce surface water reliability, and elevate post-fire hazards such as erosion and flooding, underscoring the need for integrated watershed resilience strategies.

Figure B-19. Wildfire Decadal Probability for BAU Population Scenario During Historical Period (1981 to 2010, left, %), Mid Future (2041 to 2070, center, %), and Late Future (2071 to 2100, right, %) Using Four CMIP5 Climate Models Under RCP 4.5 and RCP 8.5

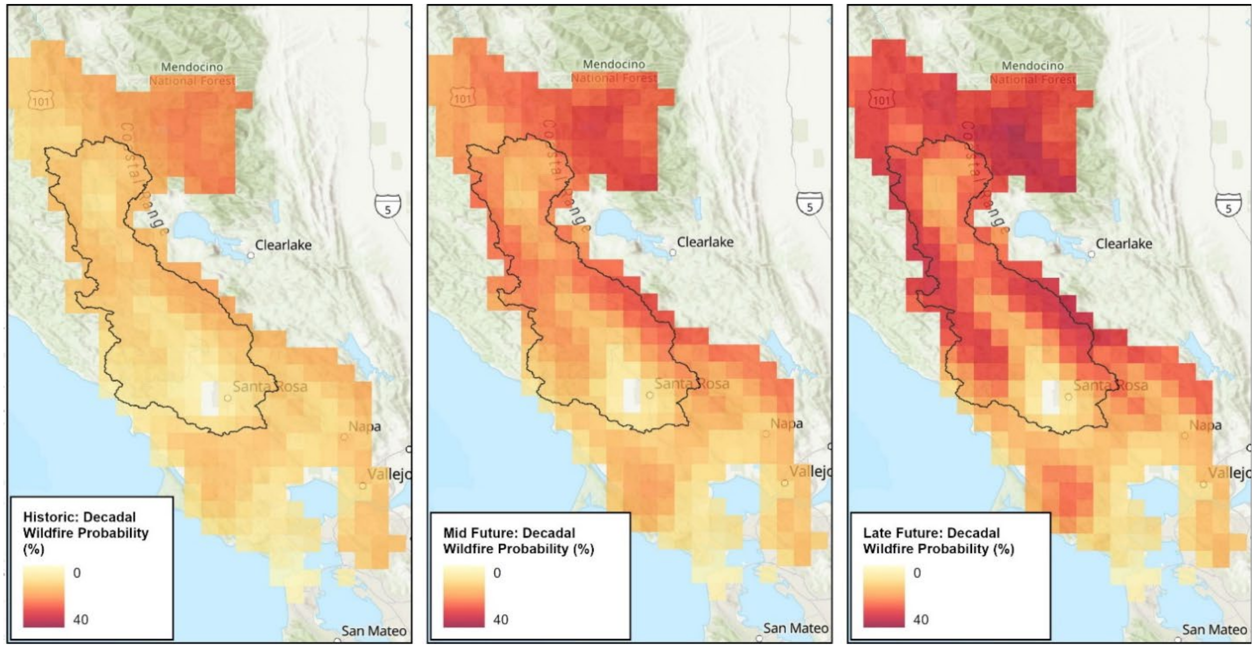

B.3.3.5 Streamflow Timing

Climate change is expected to change the streamflow timing in the future. Projected changes in streamflow timing are calculated by analyzing the following index:

- *Projected changes on the day of the year when 50% of the water-year flow has been passed*

Methodology: BCM model-simulated runoff and recharge fluxes for 15 climate models under SSP2-4.5, SSP3-7.0, and SSP5-8.5 are used to estimate the change in streamflow timing. Total runoff is defined as the grid-based flow using the summation of runoff and recharge aggregated at the annual scale based on each water year. The day of the year is identified when the cumulative total runoff is equal to 50% of the water-year total flow. The median changes are calculated for mid future (2041-2070) and late future (2071-2100) periods with respect to historical period (1981-2010).

Approach

a. BCM model-simulated daily total runoff for the 270 m grids in Russian River watershed domain was estimated by grid-wise summation of the runoff and recharge from the 41 climate projections. BCM simulated runoff and recharge values are all the grids that were extracted separately for the different climate projections.

b. The cumulative total runoff for each water year was estimated using the daily total runoff. Then the 50% of the total water-year annual flow was estimated for each water year.

c. The day of the year when cumulative daily total runoff is equal to 50% of the total water-year annual flow was calculated for each water year. The calculated day of the year values were used for estimating the index values during historical (1981 to 2010), mid (2041 to 2070), and late (2071 to 2100) future periods.

d. The absolute values of the annual index during the historical, mid, and late future periods were utilized to calculate the relative change for the future periods for 41 climate projections.

e. The projected change in the total runoff was reported as the median change of the annual index from the 41 climate projections during the mid and late future.

Key Results: The projected changes in streamflow timing indicate a clear shift in runoff under future climate conditions (Figure B-20). The historical streamflow typically peaked later in the year, while mid-future and late-future scenarios exhibit advancements of several weeks, particularly across higher-elevation region of Eel River watershed. This shift reflects warming-driven reductions in snowpack and earlier snowmelt, resulting in earlier peak flows and potentially reduced water availability during late-season periods critical for ecosystems, agriculture, and water supply management.

Figure B-20. Change in the Streamflow Timing During Mid Future (2041 to 2070, center, days) and Late Future (2071 to 2100, right, days) with Respect to Historical Period (1981 to 2010, left, day of year) Using 270 m Interpolated Data from 15 CMIP6 Climate Models under SSP2-4.5, SSP3-7.0, and SSP5-8.5

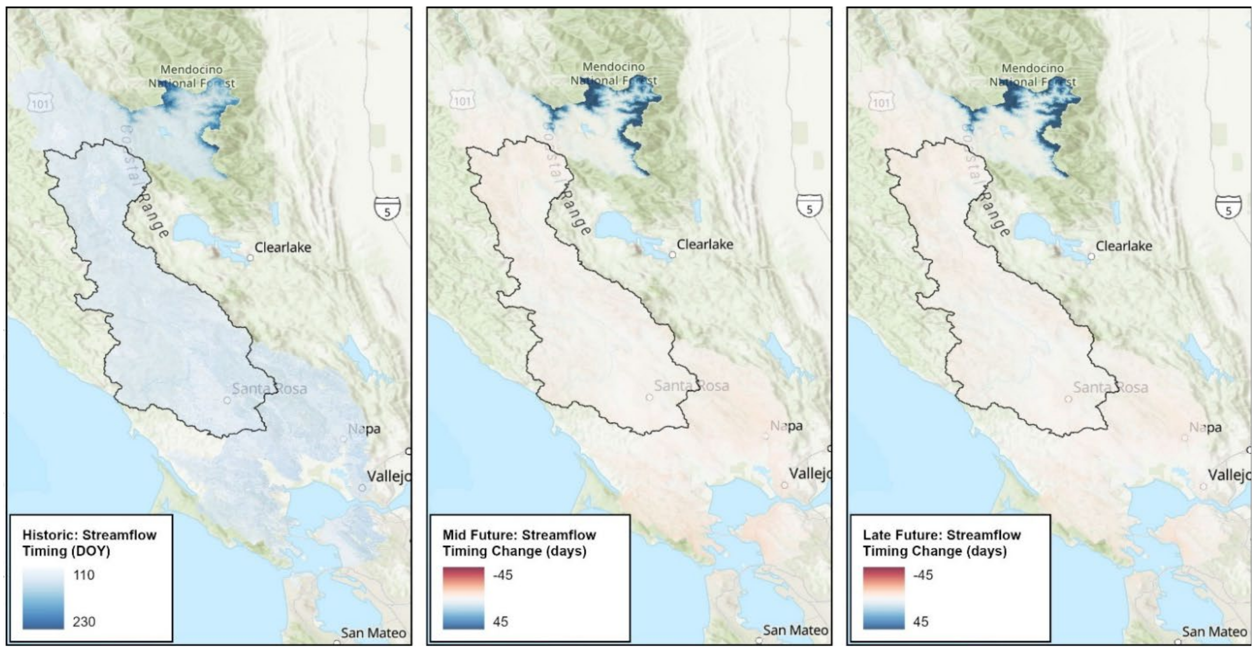

B.3.3.6 Climate Water Deficit

Climate change is expected to increase Climate Water Deficit by raising temperatures that boosts evaporative demand and reduce soil moisture. It also disrupts precipitation patterns, leading to more droughts and lower water availability, further intensifying water deficits in the future. Projected changes in climate water deficit are calculated by analyzing the following index:

- *Projected changes in climate water deficit*

Methodology: BCM model-simulated climate water deficit fluxes for 15 climate models under SSP2-4.5, SSP3-7.0, and SSP5-8.5 are used to estimate the change in annual climate water deficit. Climate water deficit is defined as the difference between potential evapotranspiration (PET) and actual evapotranspiration (AET), representing the unmet atmospheric evaporative demand. The grid-based climate water deficit was aggregated at the annual scale based on each water year. The median changes are calculated for mid future (2041–2070) and late future (2071–2100) periods with respect to historical period (1981–2010).

Approach

a. BCM model-simulated daily climate water deficit for the 270 m grids in Russian River watershed domain was extracted from the 41 climate projections.

b. The daily climate water deficit was accumulated at annual scale (October to September) for estimating the index values during historical (1981 to 2010), mid (2041 to 2070), and late (2071 to 2100) future periods.

c. The absolute values of the annual index during the historical, mid, and late future periods were utilized to calculate the relative change for the future periods for 41 climate projections.

d. The projected change in the total runoff was reported as the median change of the annual index from the 41 climate projections during the mid and late future.

Key Results: The climate water deficit is projected to increase by 5.5% during the mid future and 8.4% during the late future as compared to the historical reference value of 31 inches (Figure B-21). Projected changes in climate water deficit indicate a substantial increase in evaporative demand across the basin, driven primarily by rising temperatures and reduced soil moisture availability under future climate conditions. The mid-future scenario shows widespread increases in annual CWD, particularly in the northern and upland areas, reflecting heightened atmospheric water demand relative to available moisture. By the late-future period, these increases become more pronounced and spatially extensive, suggesting a persistent shift toward drier conditions that may intensify ecological stress, reduce water availability for vegetation, and elevate drought vulnerability across the region.

Figure B-21. Change in the Climate Water Deficit During Mid Future (2041 to 2070, center, %) and Late Future (2071 to 2100, right, %) with Respect to Historical Period (1981 to 2010, left, inch) Using 270 m Interpolated Data from 15 CMIP6 Climate Models under SSP2-4.5, SSP3-7.0, and SSP5-8.5

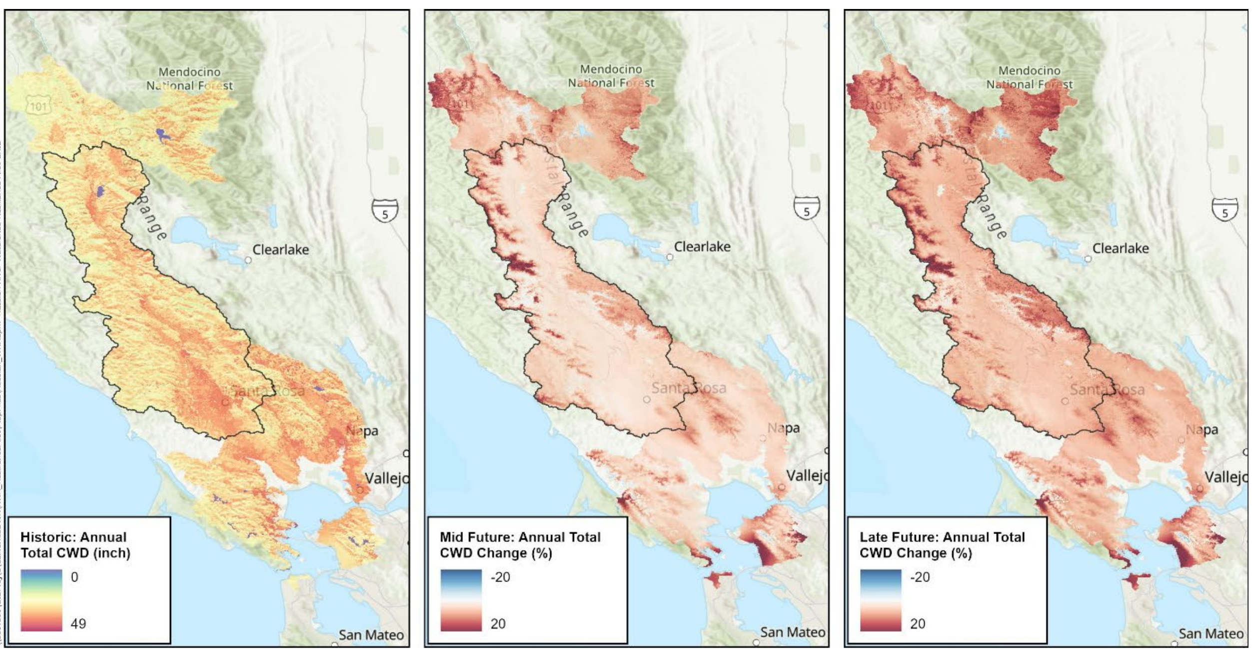

B.3.3.7 Soil Moisture

Climate change is expected to decline soil moisture due to rising temperatures that increase atmospheric evaporative demand and shifts in precipitation that reduce water availability. Projected changes in soil moisture are calculated by analyzing the following index:

- *Projected changes in soil moisture during June-August*

Methodology: BCM model-simulated soil moisture storage fluxes for 15 climate models under SSP2-4.5, SSP3-7.0, and SSP5-8.5 are used to estimate the change in soil moisture. The grid-based soil moisture storage was aggregated during the summer season (June to August) for each water year. The median changes are calculated for mid future (2041-2070) and late future (2071-2100) periods with respect to historical period (1981-2010).

Approach

a. BCM model-simulated daily soil moisture storage for the 270 m grids in Russian River watershed domain was extracted from the 41 climate projections.

b. The daily soil moisture storage was accumulated at annual scale (June to August) for estimating the index values during historical (1981 to 2010), mid (2041 to 2070), and late (2071 to 2100) future periods.

c. The absolute values of the annual index during the historical, mid, and late future periods were utilized to calculate the relative change for the future periods for 41 climate projections.

d. The projected change in the total runoff was reported as the median change of the annual index from the 41 climate projections during the mid and late future.

Key Results: The soil moisture is projected to decrease by 3.1% during the mid future and 5% during the late future as compared to the historical reference value of 24 inches (Figure B-22). Projected soil moisture conditions across the Russian River watershed indicate a clear drying trend under future climate scenarios, driven primarily by rising temperatures and more frequent and prolonged drought periods. These declines have important implications for ecosystem health, wildfire susceptibility, groundwater recharge, and soil stability, as drier soils reduce vegetative resilience and increase erosion potential.

Figure B-22. Change in the Soil Moisture During Mid Future (2041 to 2070, center, %) and Late Future (2071 to 2100, right, %) with Respect to Historical Period (1981 to 2010, left, inch) Using 270 m Interpolated Data from 15 CMIP6 Climate Models under SSP2-4.5, SSP3-7.0, and SSP5-8.5

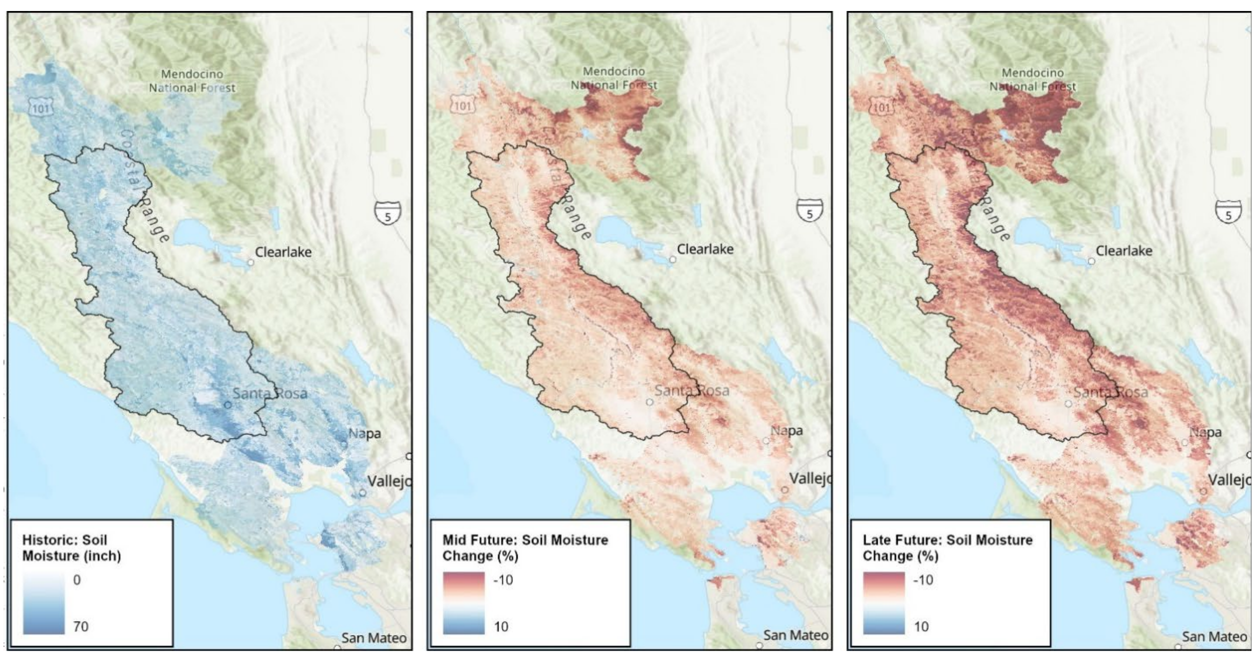

B.4 Summary

The Pilot evaluates paleo-hydrologic, historical, and future climate conditions to understand how temperature, precipitation, hydrology, and related hazards are evolving across the watershed. The assessment shows that the region has already experienced substantial climate-driven shifts, including more frequent temperature extremes, highly variable precipitation, and some of California's most intense flood and drought events.

Long-term records indicate clear warming trends, heightened climate variability, and significant sensitivity of hydrology to natural and anthropogenic climate drivers. Paleo-reconstruction results extend this perspective to more than four centuries, revealing droughts and floods of greater duration and magnitude than those captured in the instrumental record, underscoring the watershed's exposure to wide natural variability.

Future climate projections based on CMIP6 LOCA2-Hybrid downscaling show consistent increases in temperature, extreme heat days, extreme precipitation, climate water deficit, drought severity, and wildfire probability across mid- and late-century periods. Annual average temperatures are projected to rise by 3.7°F by mid-century and 6°F by late century, while extreme heat days are expected to more than double relative to historical conditions. Precipitation is projected to increase modestly overall, but extreme storms intensify considerably, contributing to higher flood risk.

Hydrologic modeling using the BCM indicates modest changes in annual runoff but substantial increases in hydrologic volatility, including enhanced flood magnitudes, earlier seasonal streamflow timing, and elevated drought severity. These patterns reflect interactions among warming temperatures, shifts in seasonal precipitation, earlier snowmelt, and increased evaporative demand. The analysis highlights that future droughts are expected to exceed historical events in severity, duration, and frequency. Wildfire projections indicate significant increases in decadal wildfire probability, rising from historical averages of 13% to 18% by mid-century and 22% by late century, reflecting the combined influence of warming, drying soils, and more persistent drought conditions. Soil moisture is projected to continue declining, further elevating ecological stress, fire risk, and erosion potential.

Overall, the combined evidence from paleo records, historical observations, and future climate projections reveals that the Russian River watershed is expected to face increasing climate-related hazards, including more extreme floods, more frequent and severe droughts, hotter temperatures, heightened wildfire risk, and altered hydrologic timing. These findings highlight the need for adaptive, integrated water-resource and watershed-resilience strategies to ensure long-term ecological, infrastructural, and water-supply reliability across the region.

B.5 References

Sonoma Water. 2024. Sonoma Countywide Flood Risk Management Assessment Update. County of Sonoma. Spring 2024. https://www.sonomawater.org/media/PDF/Water%20Resources/Flood%20Protection/Advisory%20Committees/2024/Flood%20Zone%202A%20Spring2024.pdf.

Center for Western Weather and Water Extremes. 2021. Distribution of Landfalling Atmospheric Rivers Over the U.S. West Coast during Water Year 2021: End of Water Year Summary. Scripps Institution of Oceanography. https://cw3e.ucsd.edu/cw3e-event-summary-19-26-october-2021/.

California Department of Insurance. 2024. Impacts of Extreme Heat to California's People, Infrastructure, and Economy. June. https://www.insurance.ca.gov/01-consumers/180-climate-change/upload/Impacts-of-extreme-heat-to-California-s-people-infrastructure-and-economy-by-California-Department-of-Insurance-June-2024.pdf.

Cal-Adapt. 2025. *Wildfire*. https://v2.cal-adapt.org/tools/wildfire/.

Hausfather, Z. 2018. Explainer: How 'Shared Socioeconomic Pathways' explore future climate change. Carbon Brief. April 19. Retrieved from https://www.carbonbrief.org/explainer-how-shared-socioeconomic-pathways-explore-future-climate-change/.

Pierce, D.W., D.R. Cayan, S. Rahimi, and J. Kalansky. 2023. LOCA version 2 Hybrid Downscaling. Data Justification Memo for EPC-20-006 Development of Climate Projections for California and Identification of General Use Projections.

Flint, L.E., A.L. Flint, and M.S. Stern. 2021, The Basin Characterization Model—A Regional Water Balance Software Package: U.S. Geological Survey Techniques and Methods 6–H1, 85 p., https://doi.org/10.5066/P9PT36UI.

National Oceanographic and Atmospheric Administration (NOAA). 2026. Relative Sea Level Trend 9415020 Point Reyes, California. Retrieved from NOAA Tides & Currents: https://tidesandcurrents.noaa.gov/sltrends/sltrends_station.shtml?id=9415020.

Ocean Protection Council (OPC). 2024. State of California Sea-Level Rise Guidance 2024 Science & Policy Update. Sacramento, CA. June.

Sonoma Water. 2016. Fish Habitat Flows and Water Rights Project – Draft EIR. Chapter 4.5: Recreation. Available online: https://evogov.s3.amazonaws.com/185/media/165200.pdf.

Sonoma Water. 2017. Lake Mendocino Water Supply Reliability Evaluation Report. Available online: https://www.sonomawater.org/media/PDF/Environment/BiologicalOpinion/TUCP/2013/SCWA_ReliabilityReport_30apr15_Packet.pdf.

Sonoma Water. 2021. Sonoma Water Climate Adaptation Plan. October. Available online: https://www.sonomawater.org/media/PDF/Environment/Climate%20Adaptation%20Planning/SW_CAP_Final_October_2021.pdf.

Woodhouse, C. and D. Griffin. 2008. Placing Recent Droughts in a Long-Term Context with Tree-Ring Reconstructions for the Russian River Valley. Santa Rosa Workshop on Water Conditions and Drought Preparedness. Santa Rosa, California. October. https://www.treeflow.info/sites/default/files/santarosaworkshopdendro.pdf.

Attachment B-1. Summary of Key Differences Between CMIP5 and CMIP6 Results Over the Russian River Watershed

The associated changes in temperature, precipitation, extreme heat days, and extreme precipitation were compared between the Coupled Model Intercomparison Project Phase 5 (CMIP5) and Phase 6 (CMIP6) datasets. Twenty individual downscaled general circulation model (GCM) projections were selected from 10 different CMIP5 GCMs and two different representative concentration pathways (RCPs), RCP 4.5 and RCP 8.5. These 20 climate projections were downscaled using a statistical downscaling method called "locally organized constructed analogs (LOCA)" at 1/16th degree (~6 kilometers [km]) (~3.75 miles) spatial resolution by Scripps Institution of Oceanography (Pierce et al. 2014). CMIP6 represents a significant advancement in climate modeling, building on the successes of previous phases. Localized Constructed Analogs version 2 (LOCA2) improves upon the original LOCA by offering higher spatial resolution and incorporating more sophisticated methods. While LOCA provides downscaled climate projections at a 6 km resolution for most of North America, LOCA2 enhances this with a 3 km resolution specifically for California, known as LOCA2-Hybrid. The LOCA2-Hybrid dataset uses 15 GCMs that performed well over California (Pierce et al. 2023).

The summary of key differences for changes in temperature, precipitation, extreme heat days, and extreme precipitation are described using the downscaled datasets from CMIP5 and CMIP6. The results are based on the spatial average of the hydrological boundary of the Russian River watershed.

Annual Temperature

CMIP6 annual temperature increases (4.0°F) are similar to the CMIP5 annual temperature increases (3.5°F); however, results display a smaller spread across the full range of projections (Figure B1-1). The increased ranges in temperature change during the late century are attributed to both increased variability and elevated uncertainty of the models. CMIP6 data indicates that changes in temperature are influenced by greater variability in atmospheric conditions and the inherent uncertainties in climate model projections. Increases in annual temperatures have the potential to negatively impact ecosystems by raising water temperatures, potentially surpassing habitat- and species-specific thresholds in the study area. Additionally, higher temperatures can raise consumptive and evaporative demands, requiring additional water use from both surface water and groundwater sources. Warmer conditions may also raise the risk of wildfires, particularly during periods with little to no rainfall. Elevated climatic water deficit increases stress on vegetation and forests, leading to reduced growth, higher mortality rates, shifts in species composition, and decreased resilience to other stressors like pests and diseases (McIntyre et al. 2015).

Figure B1-1. Change in Annual Average Temperature for CMIP5 and CMIP6 from Historical Period for Russian River Watershed

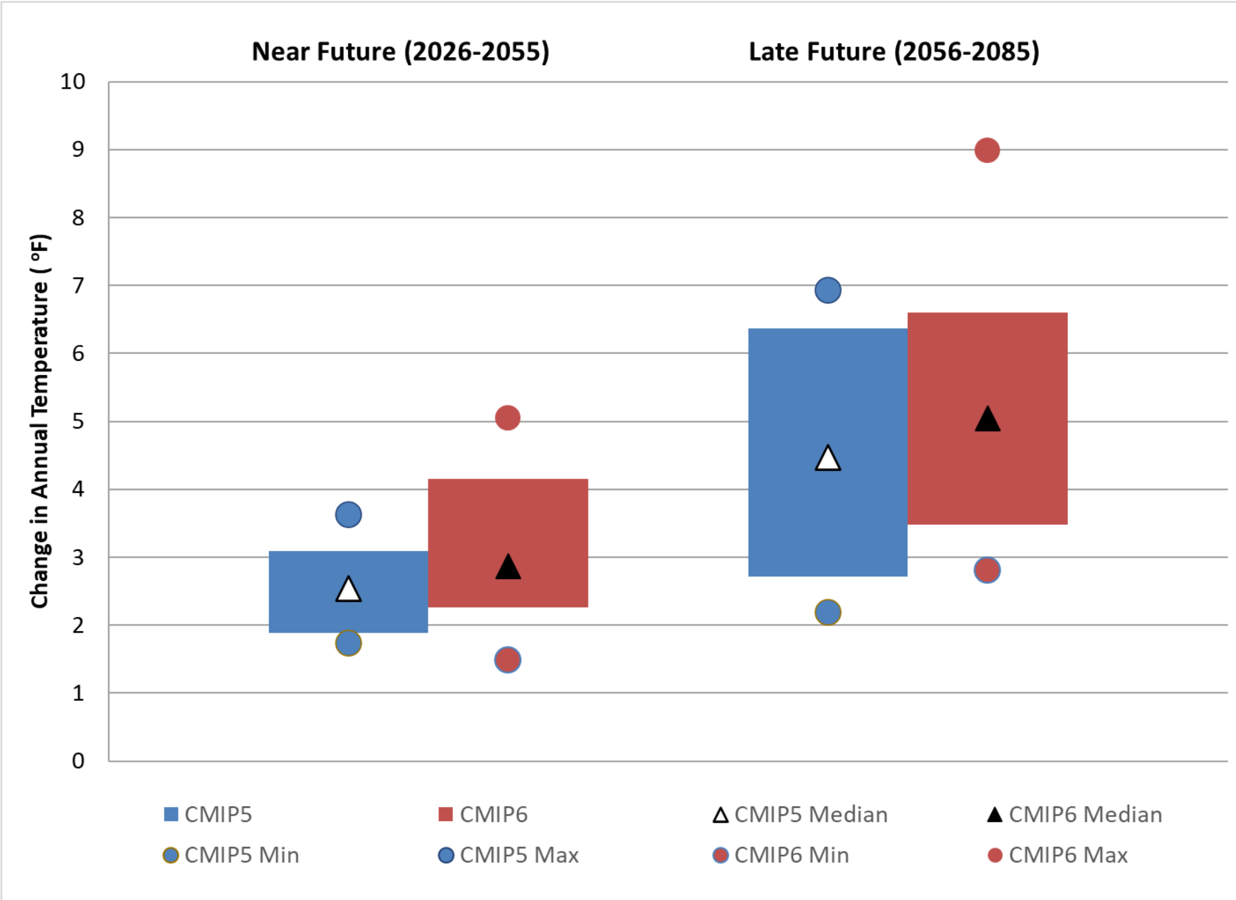

Note: The projected changes for CMIP5 and CMIP6 are computed using 20 and 129 downscaled climate model projections, simulated under RCPs 4.5 and 8.5 for CMIP5 and simulated under SSP2-4.5, SSP3-7.0, and SSP5-8.5 for CMIP6, respectively. CMIP5 and CMIP6 climate model projections have been spatially downscaled using LOCA and LOCA2-Hybrid methods at 6 km and 3 km resolution, respectively. Changes are computed with respect to 1981 to 2010 model simulated period for both CMIP5 and CMIP6. Bars represent the range between the 10th and 90th percentiles. The changes have been estimated using the values averaged over the Russian River watershed.

Seasonal Temperature

CMIP6 seasonal temperature changes are similar to the CMIP5 temperature changes for all seasons except the summer season (3.8°F under CMIP5 and 4.9°F under CMIP6) (Figure B1-2). Qualitative impacts as a result of changes to seasonal temperatures are largely consistent with those described above for annual temperature. However, species with seasonal behavioral patterns are likely to be more at risk under future climate change conditions. Additionally, seasonal agricultural demands and recreational activities may shift depending on the distribution of temperatures throughout the year.

Figure B1-2. Change in Seasonal Average Temperature for CMIP5 and CMIP6 under Near Future (top) and Late Future (bottom) Conditions Relative to Historical Period for Russian River Watershed

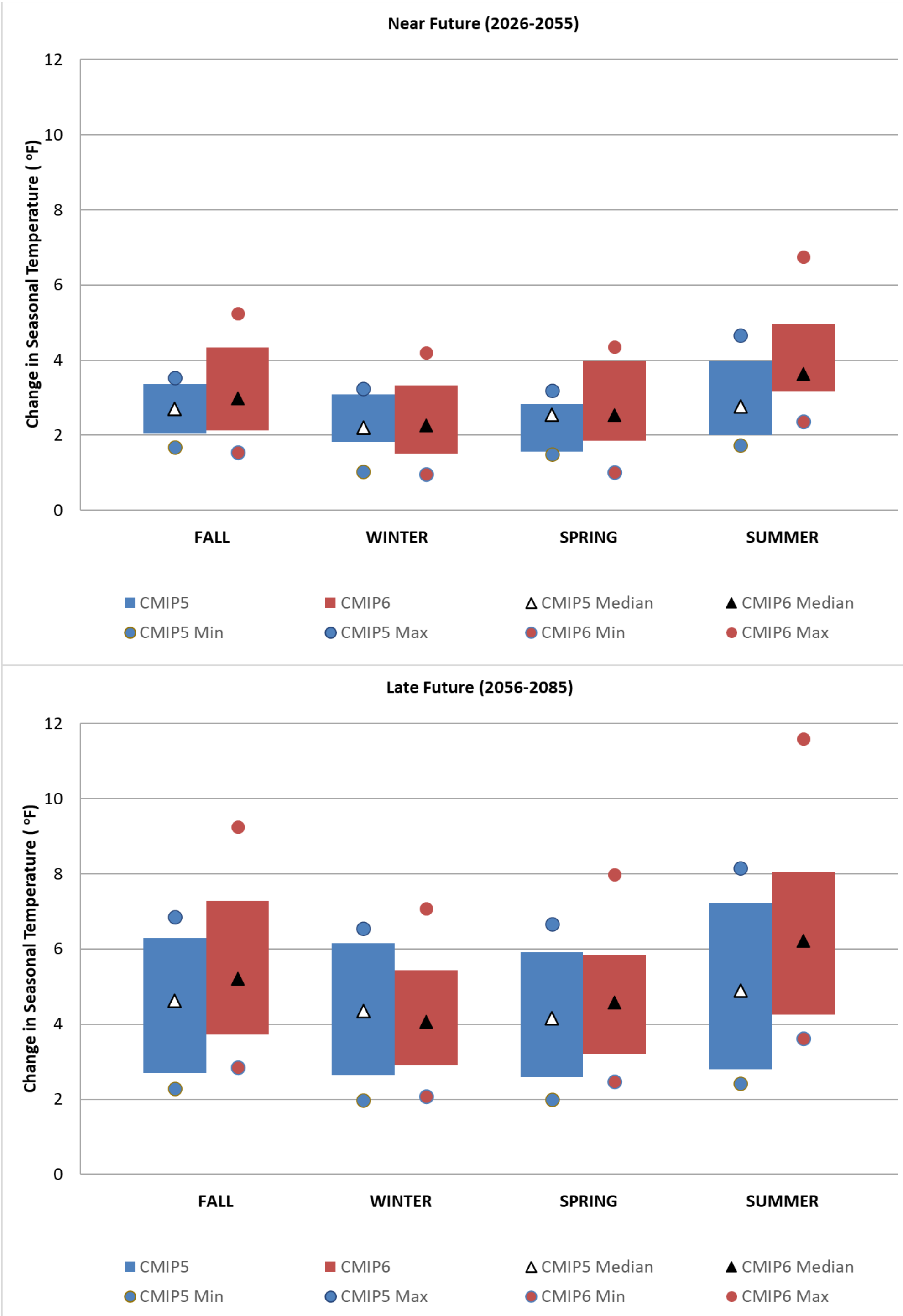

Note: The projected changes for CMIP5 and CMIP6 are computed using 20 and 129 downscaled climate model projections, simulated under RCPs 4.5 and 8.5 for CMIP5 and simulated under SSP2-4.5, SSP3-7.0, and SSP5-8.5 for CMIP6, respectively. CMIP5 and CMIP6 climate model projections have been spatially downscaled using LOCA and LOCA2-Hybrid methods at 6 km and 3 km resolution, respectively. Changes are computed with respect to 1981 to 2010 model simulated period for both CMIP5 and CMIP6. Bars represent the range between the 10th and 90th percentiles. The changes have been estimated using the values averaged over the Russian River watershed.

Annual Precipitation

CMIP6 annual precipitation changes (1.3%) are slightly lower than the CMIP5 annual precipitation changes (5.3%) (Figure B1-3). Similar to annual temperature, results display a smaller spread across the full range of projections. Annual precipitation trends appear to show a negative or near-zero change across the near future period. Decreases in precipitation can increase reliance on groundwater resources, degrade precipitation-dependent ecosystems, increase wildfire risks, and reduce the usefulness of hydropower. In the late future, increases in annual precipitation are likely to be beneficial in the absence of severe storm events. Additional precipitation may benefit surface water and groundwater supplies; however, if increases in annual precipitation are largely driven by more intense storm events, flood risks are also likely to increase. Increases in extreme precipitation and flooding can significantly impair water supply systems, including reservoirs (Devineni et al. 2015, DeFlorio et al. 2024). Increases in annual precipitation driven by more intense storms can negatively impact groundwater supplies. While intense storms may initially seem beneficial for groundwater recharge, they often lead to rapid runoff rather than infiltration. This reduces the amount of water that actually percolates into the ground to replenish aquifers (Liu et al. 2022, Dallman and Spongberg 2012).

Figure B1-3. Change in Annual Average Precipitation for CMIP5 and CMIP6 from Historical Period for Russian River Watershed

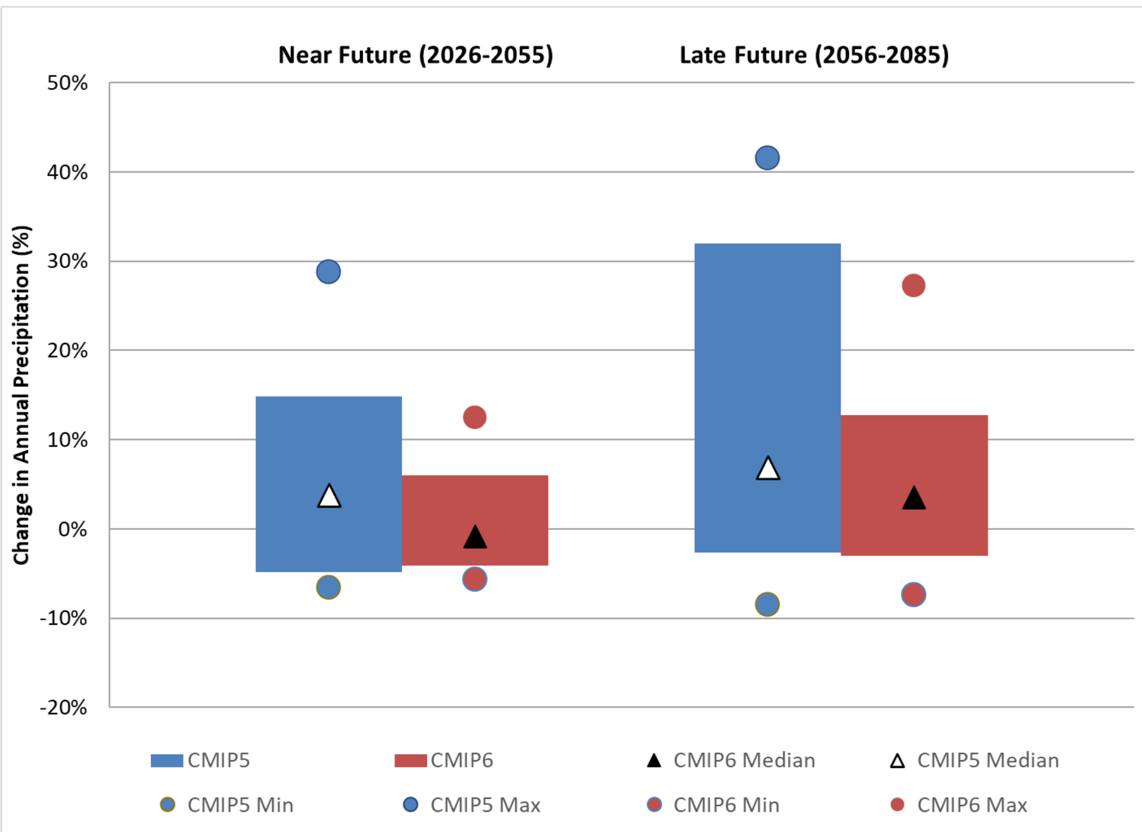

Note: The projected changes for CMIP5 and CMIP6 are computed using 20 and 129 downscaled climate model projections, simulated under RCPs 4.5 and 8.5 for CMIP5 and simulated under SSP2-4.5, SSP3-7.0, and SSP5-8.5 for CMIP6, respectively. CMIP5 and CMIP6 climate model projections have been spatially downscaled using LOCA and LOCA2-Hybrid methods at 6 km and 3 km resolution, respectively. Changes are computed with respect to 1981 to 2010 model simulated period for both CMIP5 and CMIP6. Bars represent the range between the 10th and 90th percentiles. The changes have been estimated using the values averaged over the Russian River watershed.

Seasonal Precipitation

CMIP6 precipitation changes during all seasons (-1.4%) are slightly lower than the CMIP5 seasonal precipitation changes (4.3%) (Figure B1-4). The direction of these changes (positive or negative) is the same between CMIP5 and CMIP6 except for the near future period in the summer season. Qualitative impacts as a result of changes to seasonal precipitation are largely consistent with those described above for annual precipitation and seasonal temperature. Winter is expected to experience increased precipitation, while the spring season will likely be characterized by reduced rainfall. Consequently, it is imperative to prioritize water storage and management efforts during the winter months to ensure adequate water supply throughout the drier spring period. Unlike other seasons, the spring precipitation is expected to decrease during both future periods. This anticipated reduction in rainfall could significantly impact water supply and ecosystem health, necessitating proactive measures to mitigate potential adverse effects (Polade et al. 2017, Tarín-Carrasco et al. 2024).

Figure B1-4. Change in Seasonal Average Precipitation for CMIP5 and CMIP6 under Near Future (top) and Late Future (bottom) Conditions from Historical Period for Russian River Watershed

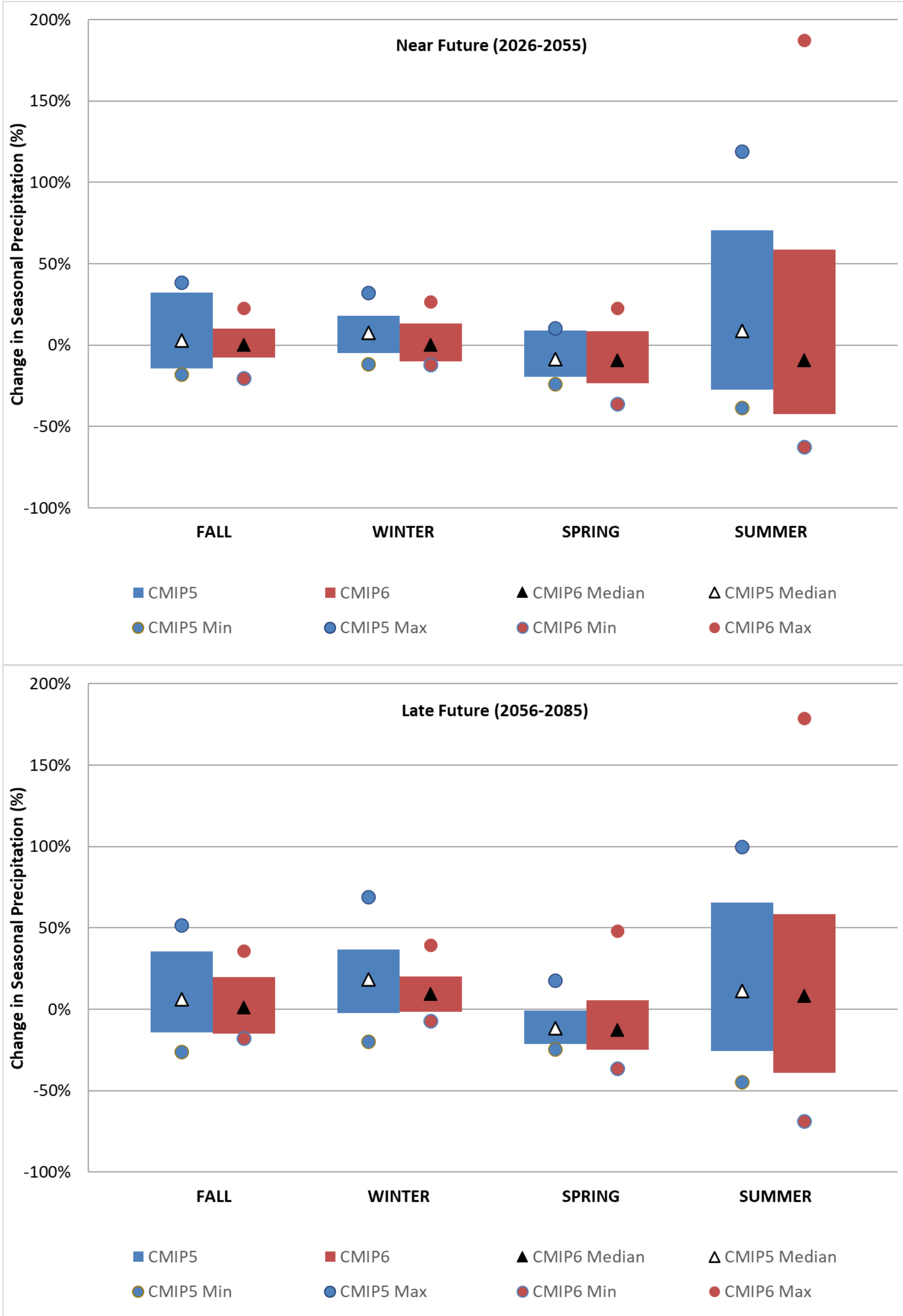

Note: The projected changes for CMIP5 and CMIP6 are computed using 20 and 129 downscaled climate model projections, simulated under RCPs 4.5 and 8.5 for CMIP5 and simulated under SSP2-4.5, SSP3-7.0, and SSP5-8.5 for CMIP6, respectively. CMIP5 and CMIP6 climate model projections have been spatially downscaled using LOCA and LOCA2-Hybrid methods at 6 km and 3 km resolution, respectively. Changes are computed with respect to 1981 to 2010 model simulated period for both CMIP5 and CMIP6. Bars represent the range between the 10th and 90th percentiles. The changes have been estimated using the values averaged over the Russian River watershed.

Extreme Heat Days

Projected trends in extreme heat days are similar under CMIP5 and CMIP6 (Figure B1-5). Extreme heat days double from the near future period (roughly 10 days) to the late future period (20 days). Increases in extreme heat days have the potential to negatively impact ecosystems for the same reasons noted above for increases in annual and seasonal temperatures. Additionally, recreational activities in the study area may decrease during periods of extreme heat, particularly for at-risk populations. The prevalence of wildfire conditions is also likely to increase during extreme heat events, especially for periods that are prolonged in nature.

Figure B1-5. Change in Annual Extreme Heat Days for CMIP5 and CMIP6 from Historical Period for Russian River Watershed

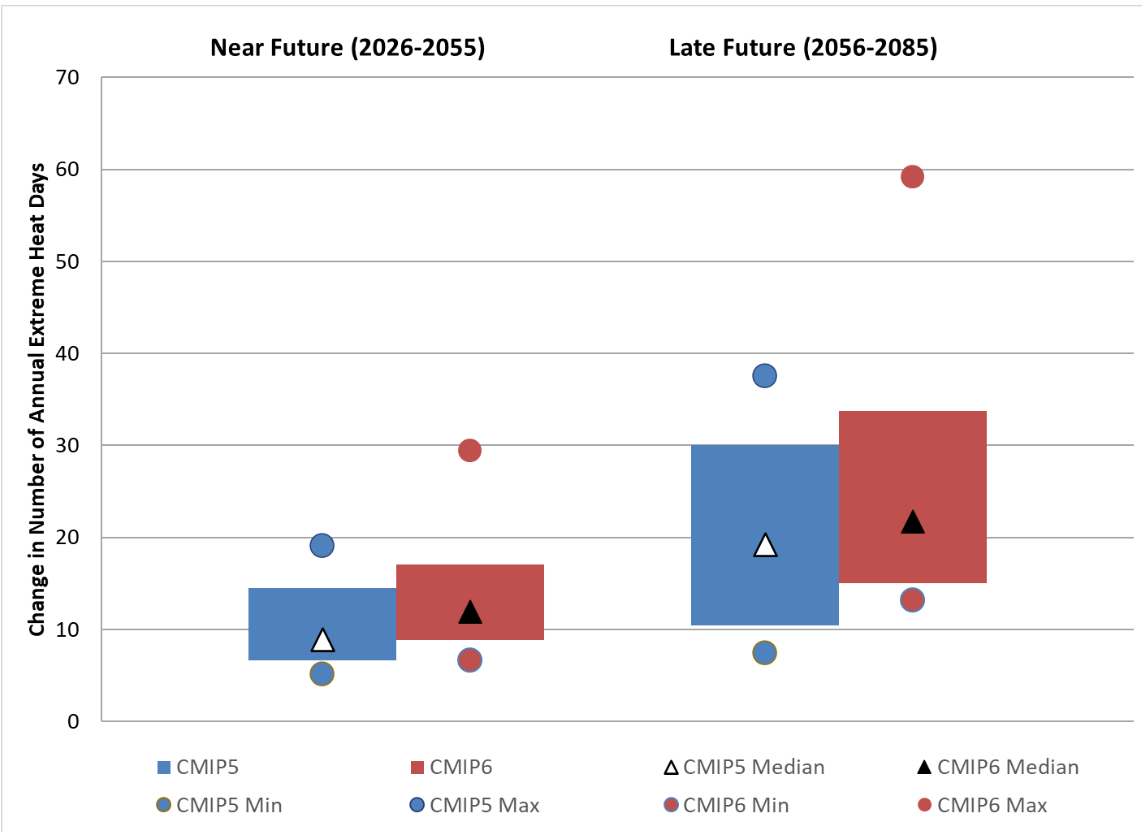

Note: The projected changes for CMIP5 and CMIP6 are computed using 20 and 129 downscaled climate model projections, simulated under RCPs 4.5 and 8.5 for CMIP5 and simulated under SSP2-4.5, SSP3-7.0, and SSP5-8.5 for CMIP6, respectively. CMIP5 and CMIP6 climate model projections have been spatially downscaled using LOCA and LOCA2-Hybrid methods at 6 km and 3 km resolution, respectively. Changes are computed with respect to 1981 to 2010 model simulated period for both CMIP5 and CMIP6. Bars represent the range between the 10th and 90th percentiles. The changes have been estimated using the values averaged over the Russian River watershed.

Extreme Precipitation

CMIP6 extreme precipitation changes (11%) are similar to CMIP5 extreme precipitation changes (13%); however, results display a smaller spread across the full range of projections (Figure B1-6). Increases in extreme precipitation events are the primary driver for increases in flood risks in the study area. With sufficient storage and operational flexibility, some of this excess precipitation may be captured for more beneficial uses (e.g., groundwater recharge).

Figure B1-6. Change in Annual Extreme Precipitation for CMIP5 and CMIP6 from Historical Period for Russian River Watershed

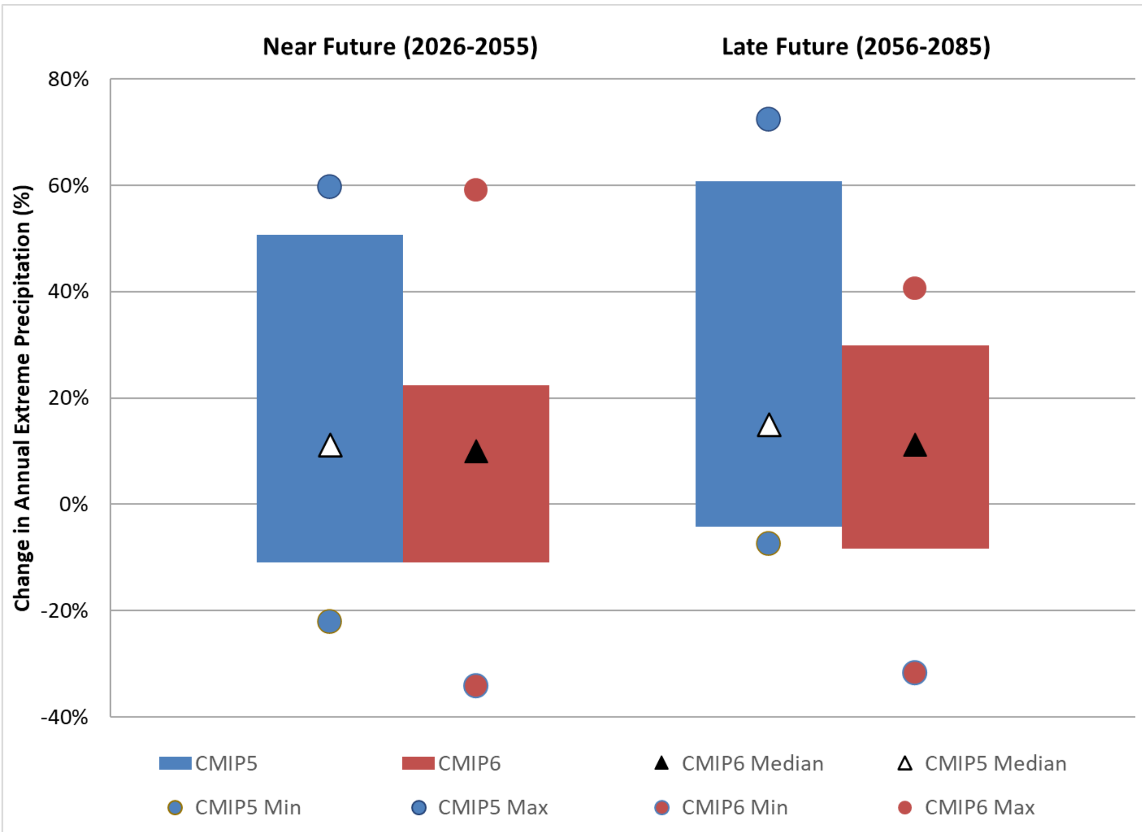

Note: The projected changes for CMIP5 and CMIP6 are computed using 20 and 129 downscaled climate model projections, simulated under RCPs 4.5 and 8.5 for CMIP5 and simulated under SSP2-4.5, SSP3-7.0, and SSP5-8.5 for CMIP6, respectively. CMIP5 and CMIP6 climate model projections have been spatially downscaled using LOCA and LOCA2-Hybrid methods at 6 km and 3 km resolution, respectively. Changes are computed with respect to 1981 to 2010 model simulated period for both CMIP5 and CMIP6. Bars represent the range between the 10th and 90th percentiles. The changes have been estimated using the values averaged over the Russian River watershed.

Seasonal Extreme Precipitation

CMIP6 extreme precipitation changes during all seasons (9.6%) are slightly lower than the CMIP5 seasonal extreme precipitation changes (14.6%) (Figure B1-7). The direction of these changes (positive or negative) is the same between CMIP5 and CMIP6 except for the near future period in the spring season. Qualitative impacts as a result of changes to seasonal extreme precipitation are largely consistent with those described above for annual extreme precipitation.

Figure B1-7. Change in Seasonal Extreme Precipitation for CMIP5 and CMIP6 under Near Future (top) and Late Future (bottom) Conditions from Historical Period for Russian River Watershed

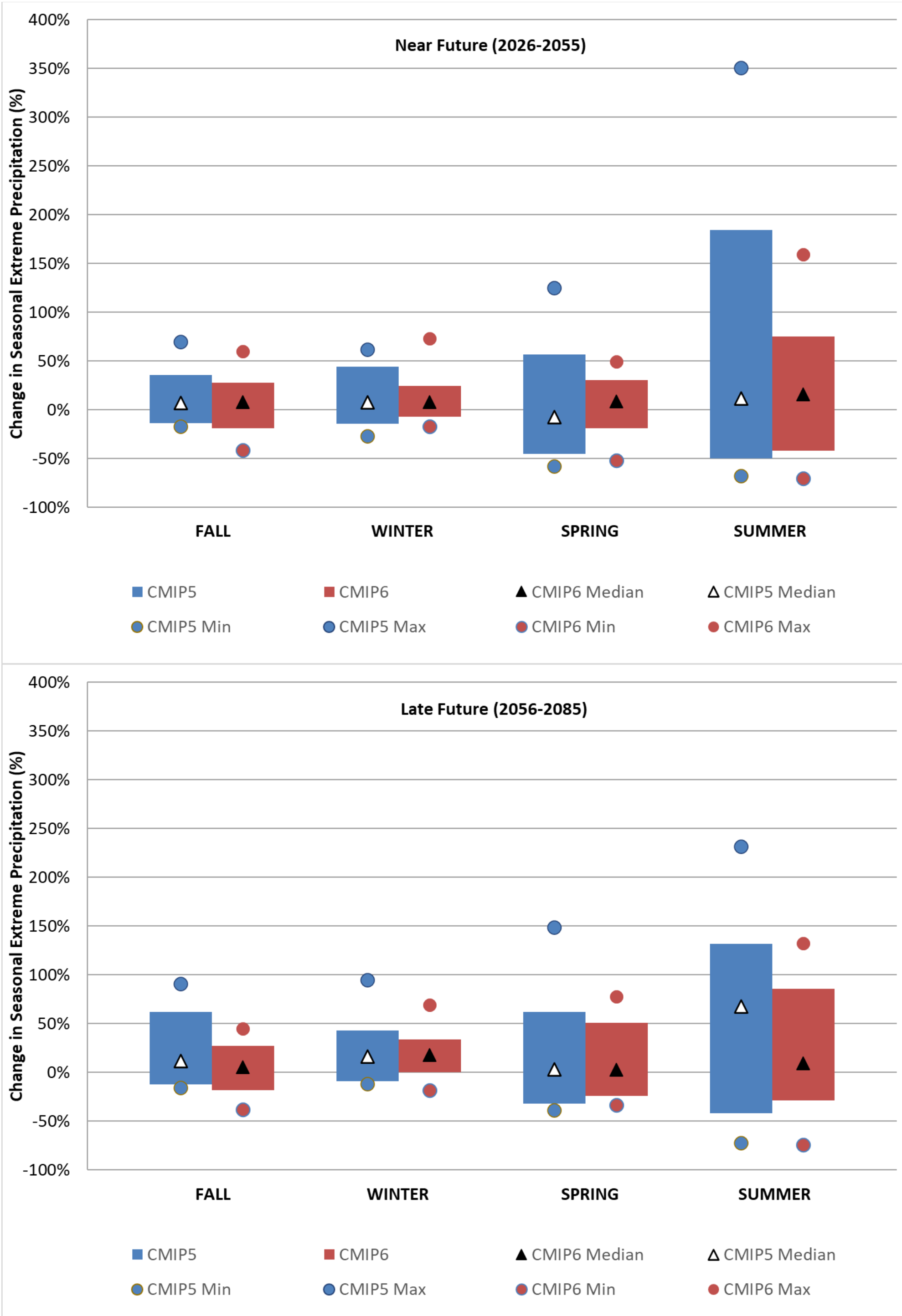

Note: The projected changes for CMIP5 and CMIP6 are computed using 20 and 129 downscaled climate model projections, simulated under RCPs 4.5 and 8.5 for CMIP5 and simulated under SSP2-4.5, SSP3-7.0, and SSP5-8.5 for CMIP6, respectively. CMIP5 and CMIP6 climate model projections have been spatially downscaled using LOCA and LOCA2-Hybrid methods at 6 km and 3 km resolution, respectively. Changes are computed with respect to 1981 to 2010 model simulated period for both CMIP5 and CMIP6. Bars represent the range between the 10th and 90th percentiles. The changes have been estimated using the values averaged over the Russian River watershed.